

Original paper

# Late Paleozoic and Early Mesozoic rare-metal granites in Central Mongolia and Baikal region: review of geochemistry, possible magma sources and related mineralization

Viktor ANTIPIN<sup>1</sup>, Ochir GEREL<sup>2\*</sup>, Alexander PERPELOV<sup>1</sup>, Dashdorjgochoo ODGEREL<sup>3</sup>, Tsegmed ZOLBOO<sup>1</sup>

<sup>1</sup> Vinogradov Institute of Geochemistry, Favorsky 1a, Irkutsk, Russia

<sup>2</sup> Mongolian University of Science and Technology, Baga Toiruu 34, Ulaanbaatar, Mongolia; gerel@must.edu.mn

<sup>3</sup> Institute of Paleontology and Geology, Mongolian Academy of Sciences, Peace Avenue 62, Ulaanbaatar Mongolia

\*Corresponding author



The Central Asian Orogenic Belt (CAOB) was a scene of intense granitoid magmatism during the Phanerozoic with formation of vast batholiths: Angara-Vitim and Daurian-Khentei. In the Late Paleozoic and Early Mesozoic times, the peripheral zones of batholiths underwent granitic magmatism associated with rare-metal mineralization. Petrological and geochemical studies show that the rare-metal Li–F granites formed, with a gap about 100 My, large igneous provinces of the Mongol–Okhotsk Belt.

Late Paleozoic rare-metal granites build a series of multiphase plutons in the Baikal region (e.g. Kharagul  $318 \pm 7$  Ma, Bitu-Dzhida  $311 \pm 10$  Ma and Urugudei  $321 \pm 5$  Ma). The early medium-grained biotite granites and leucogranites were followed by topaz-bearing microcline- and amazonite–albite granites and a series of dikes. The Early Mesozoic epoch was marked by the formation of the Daurian-Khentei Batholith (230–190 Ma) in the center of area and rifting zones with alkaline and rare-metal granite plutons on the peripheries. In contrast to the Late Paleozoic, small Early Mesozoic intrusions (e.g., Avdar Pluton  $\sim 10$  km<sup>2</sup>, 212–209 Ma) of rare-metal Li–F granites within the Avdar-Khoshutul series of granitoids coexisted with sizable plutons (e.g., Janchivlan Pluton  $\sim 70$  km<sup>2</sup>, 227–195.3 Ma). Rare-metal Li–F granites of the Janchivlan Pluton produced small domal intrusions composed of microcline–albite, amazonite–albite and albite–lepidolite granites. The Sn–Ta–Nb mineralization is associated with albite–lepidolite granites.

The rare-metal granites of the Baikal region and Central Mongolia of contrasting ages show an identical geochemical signature of Li–F granites. It is expressed by increase in F, Li, Rb, Cs, Sn, Be, Ta and Pb and decrease in Sr, Ba, Zn, Zr, Th and U contents in course of multiphase intrusions formation. The geochemical data confirm the magmatic model for genesis of the studied rare-metal Li–F granites. However, this process of magma differentiation was terminated with formation of albitites, microclinites and muscovite greisens. The whole-rock geochemistry and isotopic composition of the granites points to the Precambrian crust of the Baikal region ( $T_{2DM} = 1.0\text{--}1.3$  Ga) as the most likely source. We propose the formation of the initial granitic melts due to anatexis of the higher levels of the continental crust, with fluids released during granulite-facies metamorphism in the lower crust. The rare-metal Li–F granites of the studied provinces are intraplate formations geochemically different from the Early Paleozoic collisional granitoids. This could be caused by the influence of deep-seated source on the occurrence of rare-metal magmatism.

**Keywords:** rare-metal granites, Li–F granite, Late Paleozoic, Early Mesozoic, Mongolia, Baikal region

**Received:** 22 September, 2015; **accepted:** 26 February, 2016; **handling editor:** K. Schulmann

## 1. Introduction

Rare-metal granitoids have a distinct place in the Central Asian Orogenic Belt (CAOB) or Altaids (e.g., Şengör et al. 1993; Kovalenko et al. 1999), a large accretionary complex surrounded by the Siberian Craton to the west and the North China with Tarim cratons to the south (Kovalenko et al. 2004; Windley et al. 2007). The CAOB is characterized by intense Phanerozoic granitoid magmatism, including post-orogenic and intraplate granitoids of Late Paleozoic–Early Mesozoic age that form large batholiths, (e.g. Angara-Vitim, Daurian-

Khentei) surrounded by rift zones with bimodal basalt magmatism, subalkaline and alkaline granite plutons and rare-metal granites (Fig. 1). The origin of this large granitoid province is still controversial. Some researchers (Jahn et al. 2004, 2009) have suggested a role of juvenile component in granitoid origin. Others (Yarmolyuk et al. 2013, 2014) ascribed the major role to an activity of a mantle plume, triggering the intraplate magmatism, interaction between asthenospheric and lithospheric mantle, continental collision, and melting of crustal rocks. After Li et al. (2013) the early Mesozoic granitoids originated during subduction processes and

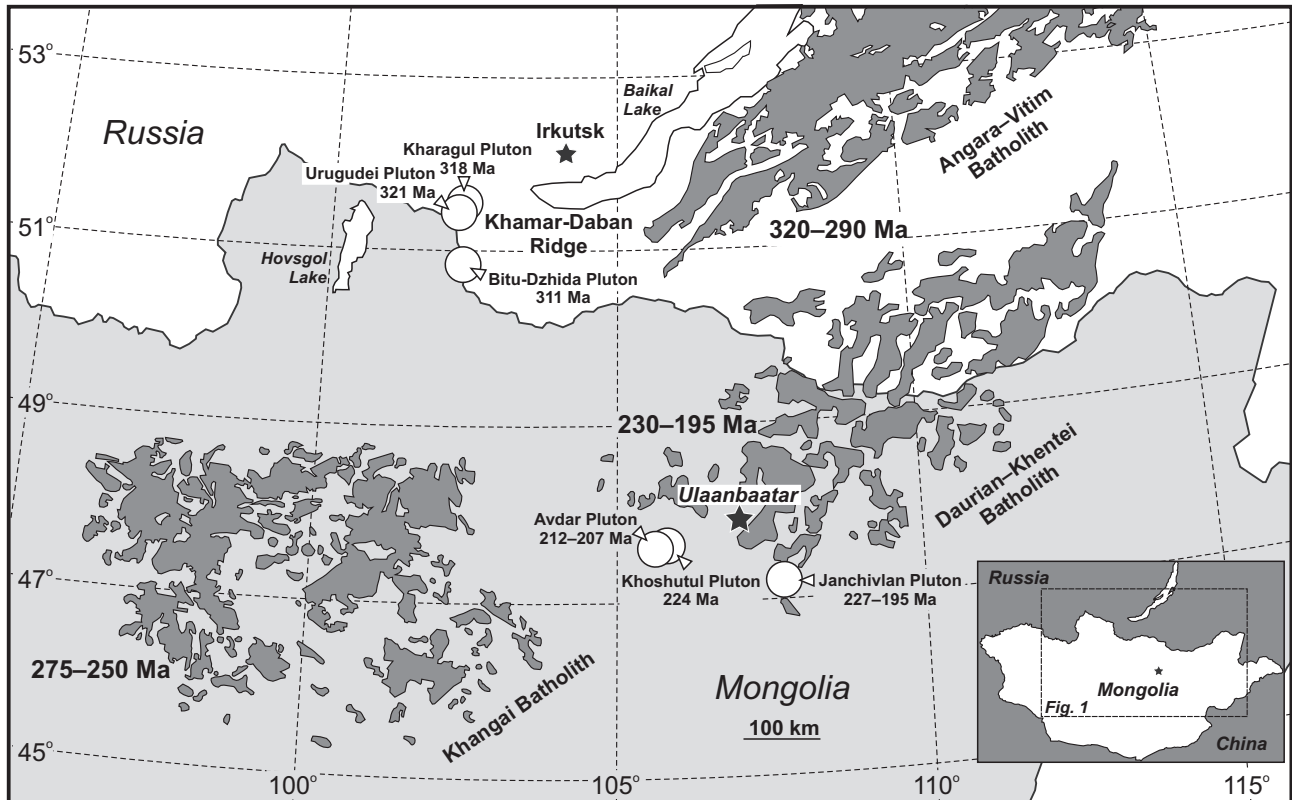


**Fig. 1** Position and the age of the studied Late Paleozoic and Early Mesozoic rare-metal granitoids and large batholiths of Central Mongolia and Baikal region, after Yarmolyuk and Kovalenko (2003). The large granite batholiths are shown in gray, rare-metal granitic plutons by white circles. Coordinates of plutons: Kharagul – N 51° 26', E 102° 11'; Urugudei N 51° 23', E 102° 12'; Bitu-Dzhida N 51° 03', E 102° 11'; Avdar N 47° 37', E 105° 27'; Janchivlan N 47° 33', E 107° 35'.

formed in active continental margin or back-arc environment (Donskaya et al. 2013).

Rare-metal granites are identified as those with high concentrations of F, Li, Rb, Cs, Be, Sn, W, Ta, Nb, Zr, and REE (Tauson 1977; Kovalenko 1977, 1978) and the metallogenically specialized granites (Tischendorf and Palchen 1985). There is a number of classification schemes of these granites. Kovalenko (1977) and Tauson (1977) recognized two different geochemical types of rare-metal granites, peralkaline (agpaitic) and metaluminous to peraluminous (plumasitic or Li–F). Each of these granite types has a distinctive set of trace-element characteristics and associated mineral deposits. The Li–F granites are enriched in Li, Rb, Ta, Sn, U, and F whereas the peralkaline granites are extremely enriched in Zr, Nb, LREE and F. In general, the peralkaline rare-metal granites appear to be part of the anorogenic group of granites (A-type) identified by Loiselle and Wones (1979), Collins et al. (1982), and Whalen et al. (1987).

After Linnen and Cuney (2005), there are three types of rare-metal granites: (1) peralkaline rare-metal granites characterized by very high abundances of F, REE, Y, Zr and Nb and high concentrations of Th, Sn, Be, Rb and U, high Nb/Ta ratios and low P contents

that are rich in Fe and emplaced in anorogenic settings; (2) metaluminous rare-metal granites typically having intermediate REE, Y, Zr, Hf and Th, associated with high-K calc-alkaline magma series and occurring in postorogenic and anorogenic settings; (3) peraluminous rare-metal granites, known as Li–F granites (Kovalenko 1977), having highly variable mineralogy, low Zr/Hf and Nb/Ta ratios, and forming postorogenic plutons in continental collision belts.

Despite numerous experimental and geochemical works as well as fluid-inclusion studies (Kovalenko 1977; Christiansen et al. 1988; Taylor 1992; Štemprok and Seltmann 1994; Dostal and Chatterjee 1995; Raimbault et al. 1995; Reyf et al. 1999; Antipin et al. 1999, 2011; Kostitsyn 2001; Badanina et al. 2010; Gu et al. 2010), the origin of Li–F granites is still open to discussion. The debate concerns the sources of granite magma, mechanism of enrichment in rare elements, and role of fluids in ore concentration. The Li–F granites typically represent the latest pulses of multiphase late/postorogenic to anorogenic granite complexes.

The discovery of subvolcanic and volcanic glassy equivalents of the topaz-bearing granites – ongonites (Kovalenko and Kovalenko 1976; Kovalenko 1977) char-

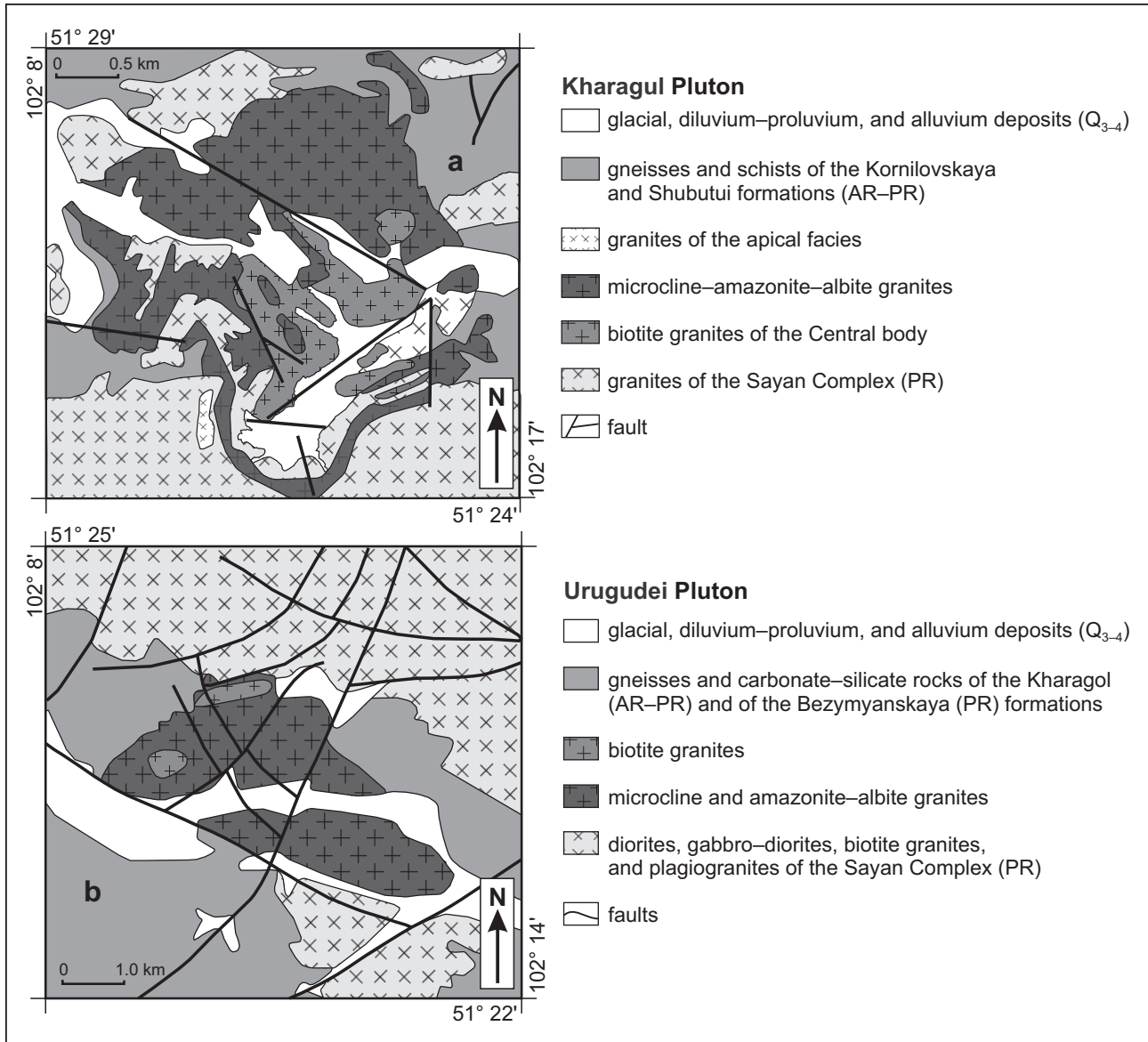


Fig. 2 Schematic geologic structure of the Kharagul (a) and Urugudei (b) rare-metal granitoid plutons (Antipin and Perepelov 2011).

acterized by enrichment of Li, Rb and Cs and related ore elements (Sn, W, U, Nb and Ta), provides strong support for the magmatic model. In this paper we discuss the geochemistry, magma sources and rare-metal mineralization of granites occurring in the Late Paleozoic and Early Mesozoic granitoid areas surrounding the Angara-Vitim and Daurian-Khentei batholiths in Central Mongolian and Russian tracts of the CAOB.

## 2. Geological setting and petrography

Late Paleozoic rare-metal granites (e.g. Kharagul, Urugudei and Bitu-Dzida) occur in the Baikal region, Russia and Early Mesozoic granites (e.g. Janchivlan and Avdar

in the marginal part of the Daurian-Khentei Batholith, Mongolia (Fig. 1)<sup>1</sup>.

### 2.1. The Kharagul Pluton

The Kharagul and Urugudei plutons are situated in the western part of the Khamar-Daban Ridge near the Urugudei peak (2758 m). The rock exposures range from 8 to 10 sq. km and both can be classed as multiphase

<sup>1</sup> In this paper we use not widely accepted names for granite rocks proposed by Kovalenko et al. (1971). Those composed predominantly of K-feldspar and albite, with accessory amounts of Li-mica, are termed "microcline–albite and amazonite–albite". If mica content exceeds 1 vol. %, granites are named "lepidolite–albite or zinnwaldite–albite", as appropriate.

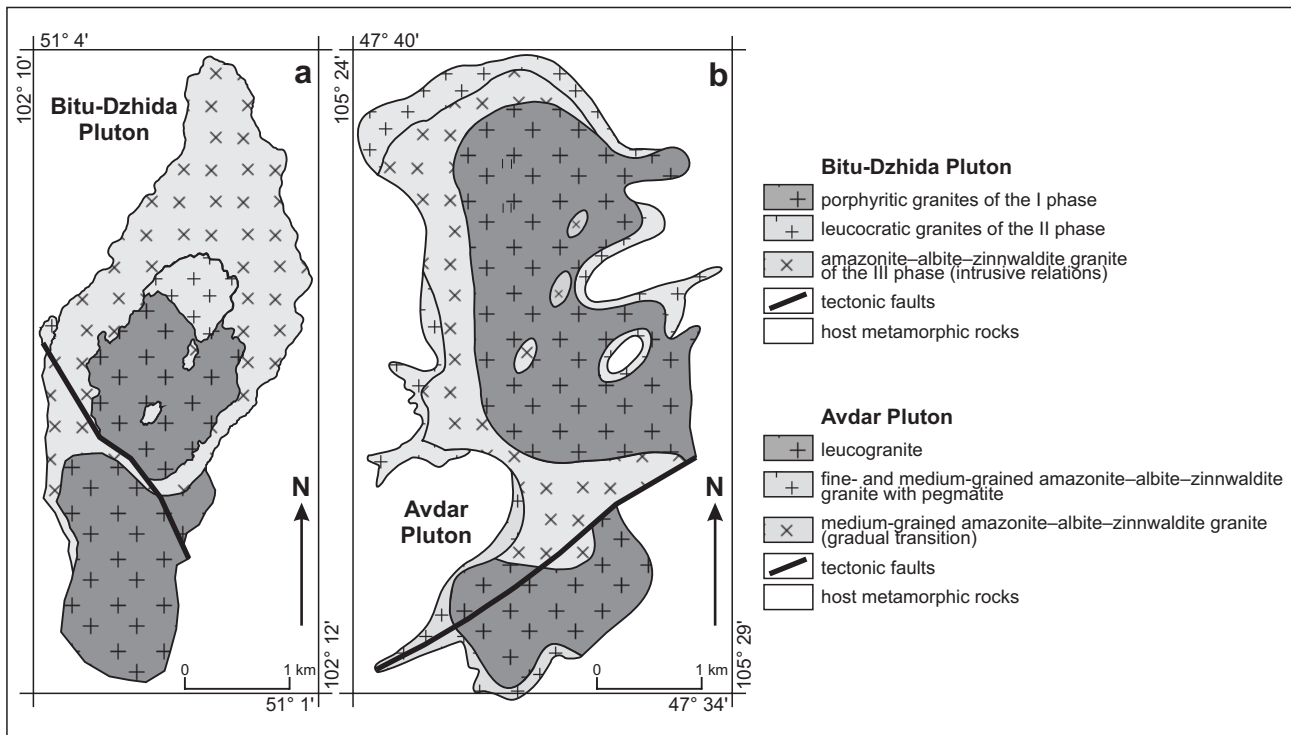


**Fig. 3** Schematic geologic structure of the Bitu-Dzhida (Antipin and Perepelov 2011) (a) and Avdar (Kovalenko et al. 1971; Antipin 1977) (b) rare-metal granite plutons.

intrusions. The Kharagul Pluton (Fig. 2a) shows a more complicated structure and greater diversity of petrographic rock types. It is an intrusive body surrounded by a series of dikes within the metamorphic rocks of the Khamar-Daban Group of the Riphean age in which the Shubutui and Kornilovskaya flysch formations are distinguished. The early intrusive phase is formed by medium- to fine-grained, in places porphyritic, biotite granites that grade into quartz syenites. In addition to feldspars, quartz, and biotite, the early granites contain fluorite (up to 1.4 vol. %) and magnetite (up to 1.2 %). The late phase in the northern part of the Kharagul Pluton is made up of medium-grained topaz-bearing microcline and amazonite–albite granites forming an intrusion extending nearly E–W. It is accompanied by a series of dikes, most of which occur among the country-rock gneisses and schists and are probably apophyses of the deep part of the pluton not exposed on surface. The largest of the dikes is 3 km long and has a thickness ranging from 15 to 70 m.

The feldspars of the late granites are cross-hatched microcline and albite ( $Ab_{3-7}$ ), and the micas are Li varieties, protolithionite and zinnwaldite, occasionally associated with lepidolite and Li phengite–muscovite in the apical part of the intrusion. In contrast to the granites of the early phase, the late rare-metal granites contain topaz (up to 1.5 vol. %), columbite–tantalite, cassiterite, and rare monazite and cyrtolite. The petrographic peculiarities of

these rocks are that the degree of quartz idiomorphism relative to other minerals is higher, albite is significantly more abundant than microcline, and topaz occurs.

## 2.2. The Urugudei Pluton

The Urugudei Pluton (Fig. 2b) is located on south slopes of the Urugudei peak and its structure is rather simple. The northern and western parts of the intrusion comprise abundant coarse- and medium-grained biotite granites, which can be assigned to the early phase. Microcline and amazonite–albite granites, which dominate at the present-day exposure level, were formed during the late-stage development of the intrusion. An important mineralogical feature of the Urugudei Pluton is the presence of 1.5–3.5 vol. % of tourmaline in both phases. It coexists with fluorite in the early biotite granites and topaz in the late amazonite–albite granites.

The two plutons of the Khamar-Daban Range have similar mineral compositions of early biotite and late rare-metal Li-mica-bearing granites (Antipin and Perepelov 2011). They differ from each other mainly by the quantitative proportions of major minerals. The biotite granites of the Urugudei Pluton are richer in quartz (by 10 vol. %) and poorer in plagioclase compared to the biotite granites of the Kharagul Pluton. The content of albite in the late amazonite–albite granites of the Urugudei intrusion is lower compared to the rare-metal granites of the

Kharagul intrusion. High contents of tourmaline, fluorite or topaz and thus, high fluorine and boron contents, are distinctive geochemical features of the magmas parental to the Urugudei granites.

### 2.3. The Bitu-Dzhida Pluton

The Bitu-Dzhida Pluton (Fig. 3a) is situated at the Russia–Mongolia border within Neoproterozoic schists of the Bitu-Dzhida Fm. The pluton is oval-shaped, curved, and elongated in a north–south direction. It is  $\sim 5 \times 2$  km in size, and its exposed area is 9 km<sup>2</sup>. Three main intrusive phases were distinguished. According to Antipin and Perepelov (2011), the first phase was Late Carboniferous ( $311 \pm 10$  Ma, whole-rock Rb–Sr method). The first phase is represented by small outcrops in the Russian part of the Pluton and considerable exposures of medium-grained and porphyritic biotite granites in Mongolia. The second phase is made up of leucocratic granites. The amazonite–albite–zinnwaldite rare-metal granites of the final, third phase are most abundant at the present-day erosion level in the Russian part of the Pluton. Fluorite occurs in some granites of all the phases and pegmatoid amazonite–albite granites (Fig. 4). Topaz is rare and was found only in the final-stage magmatic products. The development of the multiphase intrusion was closed by pegmatite formation and greisenization. The Bitu-Dzhida Pluton can be assigned to the same age group as the Urugudei (whole rocks, Rb–Sr method,  $321 \pm 5$  Ma) and Kharagul (whole rocks, Rb–Sr method,  $318 \pm 7$  Ma) plutons of rare-metal granites in the Khamar-Daban Range.

### 2.4. The Avdar Pluton

The Avdar Pluton (Fig. 3b) is located *c.* 150 km from Ulaanbaatar at the southwestern continuation of the Khoshutul Pluton and the accompanying series of dike rocks (Fig. 1). The Khoshutul Pluton is a multistage intrusion with whole-rock Rb–Sr age of  $224 \pm 10$  Ma (Odgerel and Antipin 2009). Host rocks are represented by upper and partly middle section of the Paleozoic Mandal Group.

Shape of the Avdar Pluton is elliptical, and the area of

the rock outcrops does not exceed 10 km<sup>2</sup> ( $6 \times 2.5$  km). The Avdar Pluton is located within a brachyantlinal structure, and is elongated in a longitudinal direction. The northern and eastern parts are concordant with host rocks, and western contact is sharply discordant. The internal zonal structure of the Pluton and its relationship with host rocks suggest a dome-shaped intrusion, the apical part of which is located near the top of the Avdar Uul (Kovalenko et al. 1971; Antipin 1977). The central largest area is occupied by medium-grained biotite-bearing leucogranites, rimmed in the east and north by zone of intermittent medium-grained amazonite–albite granites that also occur in the apical parts. Directly near the exocontact, narrow zone of inequigranular aplitic granite with numerous schlieren of quartz–microcline pegmatites has been observed. Contacts between different types of the Avdar granites are usually gradual. A zonal structure is reflected that the rocks in hanging inner contact are represented by pegmatoid granite with amazonite, and in its footwall they gradually pass into aplitic granites and then to felsites with chilled zones and fluidal texture.

Pelitic xenoliths within the Pluton were transformed to quartz–cordierite–andalusite–biotite–magnetite  $\pm$  plagioclase hornfelses. The highest degree of thermal metamorphism is noted in small xenoliths metamorphosed into zinnwaldite–fluorite–magnetite–quartz  $\pm$  K-feldspar hornfelses.

The first data on the age of leucogranite and amazonite–albite granite of the Avdar Pluton were obtained by K–Ar dating of biotite (172–222 Ma, five determinations of Kovalenko et al. 1971). The Rb–Sr whole rock–mineral (biotite) isochron age of  $202\text{--}205 \pm 2$  Ma (Kovalenko et al. 1999) confirms that it belongs to the Early Mesozoic magmatic stage.

Plagioclase ( $An_{4-18}$ ) in leucogranites of the Avdar Pluton accounts typically for less than 25 vol. %, and it occurs in the prismatic and small lath-shaped grains. Microcline ( $Or_{77}Ab_{23}$ ) forms rather euhedral grains

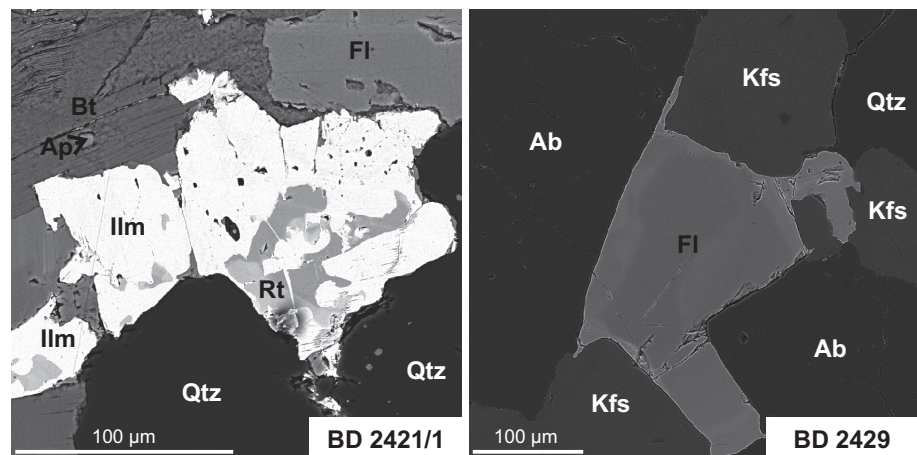


**Fig. 4** Backscattered-electron image of fluorite in granite of the first (BD 2421/1) and third (BD 2429) phases of the Bitu-Dzhida Pluton. Bt – biotite, Ab – albite, Kfs – potassium feldspar, Qtz – quartz, Ilm – ilmenite, Ap – apatite, Fl – fluorite.

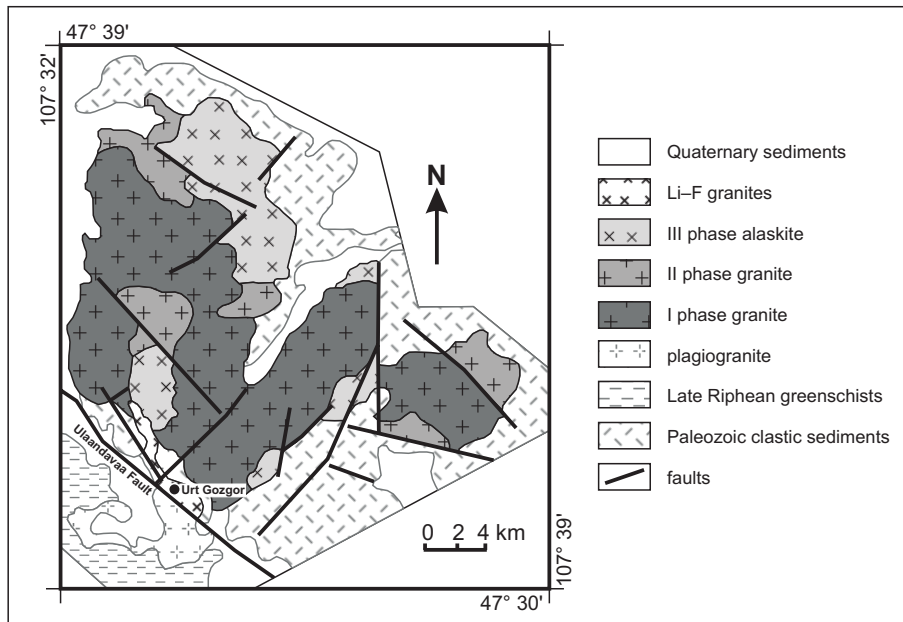


**Fig. 5** Simplified geological map of the Janchivlan Pluton (modified after Kovalenko et al. 1971).

with rough edges and contains perthites in the central parts. The total content of alkali feldspar in leucogranites approaches 35–36 %, and the amount of biotite is usually *c.* 2.5–3.0 %. Typical accessory minerals in leucogranites are magnetite, ilmenite, fluorite, zircon and monazite.

Medium-grained amazonite–albite granites have a more sodic plagioclase ( $An_{2-7}$ ) and microcline is characterized by a lower content of albite ( $Or_{81-85}, Ab_{15-19}$ ). Micas are of lithium–iron type. The amazonite–albite granites are characterized by the following accessory minerals: fluorite, zircon, ilmenite, magnetite, and columbite–tantallite.

## 2.5. The Janchivlan Pluton

The Janchivlan Pluton is located at the southern tip of the Early Mesozoic Daurian-Khentei Batholith (e.g. Kovalenko et al. 1971; Antipin 1977; Gerel 1990; Koval 1998). Marginal parts of the Batholith host small shallow intrusions of alkaline and subalkaline granite series with Li–F peraluminous rare-metal granites as the final products. These intrusions are unfoliated, discordant and surrounded by contact-metamorphic aureoles of hornfels or have tectonic contacts. The regional structure of the Daurian-Khentei Batholith is characterized by strike-slip faults that display dominant northeast trends. The Janchivlan Pluton (Fig. 5) occupies an area of about 1,100 sq. km. Host rocks consist of Precambrian quartz–chlorite–sericite schists with quartzite lenses, Middle Paleozoic sandstones and siltstones, intruded by plagiogranites of Early Mesozoic age. The main trend of the Paleozoic

structures is conformable with the strike of the Khentei synclinorium.

In the Janchivlan Pluton, Ushakov and Boguslavsky (1969) have distinguished four intrusive phases, while Kovalenko et al. (1971) listed only three main ones. Yarmolyuk et al. (2002) reported zircon U–Pb ages of  $217 \pm 52$  Ma and  $227 \pm 8$  Ma, for the first and second phases respectively and a whole-rock Rb–Sr age of  $195 \pm 0.6$  Ma for the Li–F granites (amazonite–albite granites). The Pluton shows a complicated shape with its apex directed to the northeast, the direction of the Mesozoic fault system. Faults divide the Pluton into three segments: western, central and eastern.

The dominant central part of this Pluton is composed of the first phase porphyritic coarse-grained granites with abundant miarolitic pegmatites. The second phase of equigranular medium-grained biotite and muscovite–biotite granites occur as two small outcrops in the center, and the third phase is represented by leucogranites (biotite alaskites of Kovalenko et al. 1971) that crop out in the northern and central parts of the Pluton. Lithium–fluorine granites containing amazonite–albite, microcline–albite and lepidolite–albite assemblages form small bodies which intruded in the southern part of the Janchivlan Pluton known as Urt Gozgor outcrops, controlled by the Ulaandavaa Fault in the southern part of the Pluton (Fig. 5).

Porphyritic coarse-grained biotite granite of the first phase accounts for *c.* 60 % of the intrusion. It contains K-feldspar as phenocrysts ( $Or_{75}Ab_{25}$ ) and in groundmass ( $Or_{86}Ab_{14}$ ) (45–65 vol. %), quartz (30–35 %), plagioclase  $An_{24-26}$  (10–15 %), biotite (3–5 %) and amphibole (0–2 %); allanite, apatite, zircon, magnetite and ilmenite are accessory minerals. Biotite and leucocratic granites

contain a number of miarolitic, well-differentiated pegmatites. The pegmatites are composed of quartz, K feldspar, plagioclase, and biotite, with accessory muscovite, beryl, topaz, tourmaline, zircon, allanite, magnetite, and molybdenite.

Second phase granites occupy *c.* 25 % of the intrusion outcrop and are represented by medium-grained weakly porphyritic biotite–muscovite granite composed of K-feldspar ( $\text{Or}_{75}\text{Ab}_{25}$ ; 40–45 vol. %), plagioclase  $\text{An}_{20-25}$  (10–15 %), quartz (32–25 %), biotite (4–6 %) and muscovite (2 %), with accessory allanite, apatite, zircon and magnetite.

Third-phase leucogranites (biotite alaskites) occupy *c.* 15 % of the outcrop and crop out mainly in the north-eastern part of the Pluton. They are composed of K-feldspar (36–38 vol. %), plagioclase  $\text{An}_{15-5}$  (15–23 %), quartz (38–40 %), biotite (3–4 %) and accessory minerals: topaz, fluorite, monazite, ilmenite, and magnetite. The Li–F granites are associated with the third phase. These microcline–albite and amazonite–albite granites occur in the southwestern part of the Pluton. The latter and the Urt Gozgor outcrop of rare-metal granites have asymmetric dome shapes elongated in a NW–SE direction. They occur along the large Ulaandavaa Fault and are fractured into same blocks by northeastern faults cross-cutting the Ulaandavaa Fault. Microcline–albite and amazonite–albite granites account for *c.* 6 % and lepidolite–albite granites for 1 % of the pluton. Microcline–albite granites are medium-grained rocks composed of quartz (40 vol. %), perthitic K-feldspar (30.5 %), albite  $\text{An}_{2-10}$  (25.5 %) and accessory mica: protolithionite and Li-phengite. Other accessory minerals are topaz, fluorite, zircon, monazite, columbite, xenotime, cassiterite and magnetite. Amazonite–albite granites are medium-grained, poorly porphyritic and composed of quartz (38–39 vol. %), amazonite (35 %), albite (21 %) and mica (zinnwaldite), together with accessory topaz, fluorite, zircon, monazite, columbite and cassiterite (Gerel et al. 1999).

Albite–lepidolite granites are composed of quartz (23 vol. %), albite (57 %), K-feldspar (14 %), lepidolite (4 %) and topaz (2–2.5 %). Some samples contain up to 10 % topaz and up to 20 % lepidolite. Albitites may reach even 90 % of albite, 3 % microcline, 3 % quartz, 2.5 % lepidolite and 0.4 % topaz. Accessory minerals are fluorite, zircon, monazite, columbite, Pb-pyrochlore and cassiterite. The structures range from fine-grained to porphyritic and pegmatitic (Kovalenko et al. 1971).

Albite, quartz, K-feldspar and Li-mica are the main rock-forming minerals of the Li–F granites. Magmatic topaz is a common accessory mineral. Granite is greisenized; fluorite and cassiterite are common in all types of Li–F granites. Mica forms trend from siderophyllite in the first-phase granites to zinnwaldite and lepidolite in third-phase Li–F granites.

### 3. Analytical methods

#### 3.1. Whole-rock geochemistry

Major-element oxides (wt. %) were analyzed by Multi-channel X-Ray Spectrometer SRM-25, “Orelnauchpribor”, Russia at the Center of Isotope-Geochemical Studies, Vinogradov Institute of Geochemistry, Russian Academy of Sciences, Siberian Branch (IGS SB RAS). Rh-anode has been used. The measurements were performed at a voltage of 30 kV and a current of 40 mA. Samples were homogenized by a fusion with lithium metaborate ( $\text{LiBO}_2$ ) in an induction furnace in glassy carbon melting pot at 1100 °C. The ratio of sample to flux was 1:2. The calibration was carried out using SH-1A (granite, Russia), SG-2 (granite, Russia), and JG-2 (granite, Japan) standards.

Trace elements were determined using Agilent 7700x Quadrupole ICP-MS at the “Baikal Nanotechnology Center” of the Industrial Park at the Irkutsk State Technical University. For measurements were chosen optimal conditions: plasma power of 1550 W, the reflected power 11 W, plasma gas flow 15.01 l/min; the integration time was 0.1 s per data point. Sample fusion with anhydrous lithium metaborate (1 : 4) was performed in a glassy melting pot with subsequent decomposition by a HF and  $\text{HNO}_3$  (both supra-pure (MERCK)) acid mixture. The sample weight was 100 mg, and the final dilution factor of sample solutions (3%  $\text{HNO}_3$ ) was 10,000×. The accuracy was checked using the Geological Survey of Japan standards JG-3 (granite) and JR-1 (rhyolite). Emission determination of fluorine was carried out by the Diffraction Spectrometer DFS-458S (Russia) with photodiode arrays MAES (Vasil'yeva and Shabanova 2012) using the integrated software ARDES (Spectr-Inform Ltd., Russia). Lithium was analyzed by flame photometry.

In addition, representative samples of the Janchivlan Pluton were analyzed at the Department of Geoscience, Shimane University, and Institute of Mineralogy, Petrology and Economic Geology, Tohoku University, Japan. Major-element chemical analyses were carried out using the RIX-2000 XRF, Li by ion-electrode method and Rb by atomic absorption spectrophotometry. Remaining trace elements were determined by ICP-MS Agilent 7500cs system, housed at the Shimane University, following alkali fusion and acid digestion methods, described by Kimura et al. (1995).

#### 3.2. Sr–Nd isotopes

The isotopic composition of Sr, Nd and Pb for the Bitu-Dzhida Pluton was performed at the IGS SB RAS. For isotopic analyses, 100 mg of the sample powder were dissolved in a Teflon beaker with  $\text{HNO}_3$ –HF– $\text{HClO}_4$

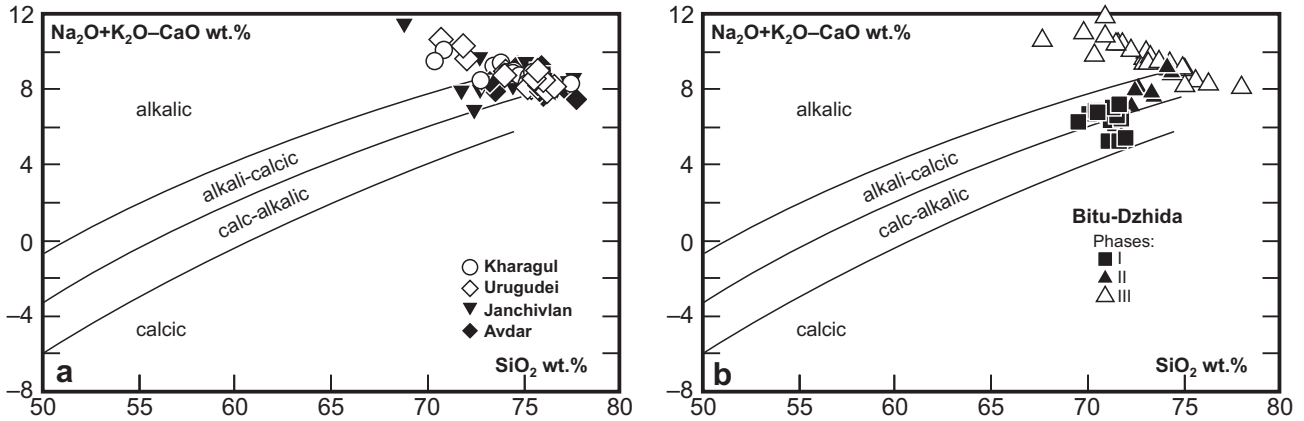


Fig. 6 Classification diagrams of Late Paleozoic and Early Mesozoic rare-metal granitoids of Central Mongolia and Baikal region in coordinates  $SiO_2$  vs.  $(Na_2O + K_2O - CaO)$  (Frost et al. 2001).

acid mixture and heated using a microwave oven. For separation of Sr and Nd, EIChrom Industries II (USA) resin was used. Separation of rare earths, Sr and Nd was performed using TRU Spec and Ln Spec resins (Pin and Zalduegui 1997). For Sr isolation, Sr Spec resin was employed (Pin et al. 1994).

The measurement of the Nd and Sr isotopic ratios was carried out by Finnigan MAT 262 Thermal Ionization Mass Spectrometer (TIMS). The accuracy of the analysis was checked by measuring the SRM 987 ( $^{87}Sr/^{86}Sr = 0.710250$  certified) and JNd-1 ( $^{143}Nd/^{144}Nd = 0.512100$  certified) standards. The values obtained in parallel experiments were:  $0.710255 \pm 15$  ( $n = 19$ ) for the SRM 987 and  $0.512101 \pm 6$  ( $n = 34$ ) for JNd-1. During mass spectrometric measurements, the isotope ratios were normalized to  $^{88}Sr/^{86}Sr = 8.375209$  and  $^{146}Nd/^{144}Nd = 0.7219$ , respectively. The  $\epsilon Nd$  values and two-stage Depleted Mantle Nd model ages ( $T_{2DM}$ ) were calculated according to Faure (1986) and Keto and Jacobsen (1987). Concentrations of Rb, Sr, Sm, Nd (ppm) were determined by the ICP-MS.

### 3.3. Pb isotopes

Isolation of Pb was achieved using the BioRad-AG1X8 resin and slightly modified procedure of Krogh (1973).

The isotopic compositions for the Bitu-Dzhida Pluton were acquired on multicollector ICP-MS NEPTUNE Plus at the IGS SB RAS using dual isotope dilution method with  $^{207}Pb + ^{204}Pb$  tracer. Optimization of the isotopic composition of the tracer is made with the advice (Galer 1999; Rudge et al. 2009). The measurements were performed with the correction for  $^{204}Hg$ . The background level did not exceed  $3 \times 10^{-15}$  A,  $^{202}Hg$  in Pb spectrum averaged  $2 \times 10^{-15}$  A. The intensity of the  $^{208}Pb$  ion current was not less than  $3 \times 10^{-11}$  A. Measurements of standard sample NIST SRM-981 ( $n = 27$ ) gave  $^{206}Pb/^{204}Pb = 16.9376 \pm 0.0022$ ;  $^{207}Pb/^{204}Pb = 15.4918 \pm 0.0022$ ;  $^{208}Pb/^{204}Pb = 36.695 \pm 0.006$ . Accuracy of analysis ( $2\sigma$ ) was 0.017–0.019 %.

For some samples of the Bitu-Dzhida Pluton Pb isotopic characteristics were obtained using a TIMS Finnigan MAT 262, considering the mass fractionation for isotopic standard NBS 981. The isotopic composition of Pb was measured in the single-mode. The correctness of the analysis was checked by measuring the standard sample SRM-981 ( $^{208}Pb/^{204}Pb = 36.722$ ,  $^{207}Pb/^{204}Pb = 15.492$ ,  $^{206}Pb/^{204}Pb = 16.937$  certified). The measured SRM-981 standard in parallel experiments gave  $36.580 \pm 0.008$ ,  $15.453 \pm 0.004$ ,  $16.908 \pm 0.005$  ( $n = 33$ ).

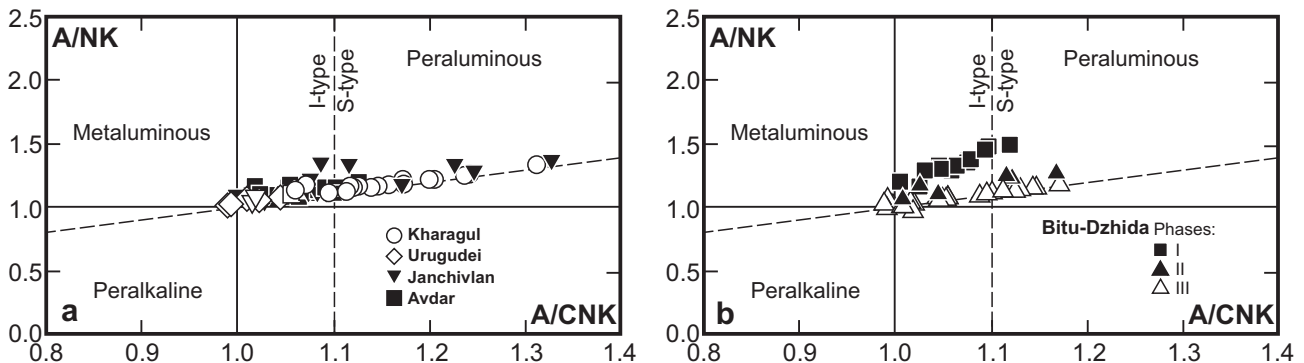


Fig. 7 The A/NK – A/CNK plot for the studied rare-metal granitoids (Shand 1943).

## 4. Whole-rock geochemistry

### 4.1. Kharagul and Urugudei plutons

The development of multiphase intrusions from early biotite granites to late amazonite–albite granites with Li–F mica was accompanied by an increase in SiO<sub>2</sub> (Fig. 6a) and, especially, Na<sub>2</sub>O contents, whereas the level of FeO, CaO, and K<sub>2</sub>O declined (Tab. 1) (Antipin and Perepelov 2011). In the same direction, i.e. from the earlier to the late granites, increase also the Al<sub>2</sub>O<sub>3</sub> contents and, accordingly, A/NK and A/CNK (Fig. 7a). Geochemical evolution included an increase in F, Li, Rb, Cs, Sn, Be, Ta, and Pb and a decrease in Ba, Sr, Zn, Zr, Th and U contents. Similar evolution is also characteristic of the subvolcanic rocks, which underlines the genetic relation of the whole intrusive–dike complex of the Khamar-Daban Province. Significant differences were detected in the distribution of K, Ba, Sr, and Zr between the calc-alkaline granitoids and rare-metal Li–F granites (Antipin and Perepelov 2011).

Kovalenko et al. (1999) reported whole-rock Rb–Sr isochron age of  $318 \pm 7$  Ma for the main granite varieties of the Kharagul Pluton with an initial <sup>87</sup>Sr/<sup>86</sup>Sr isotopic ratio  $0.711 \pm 0.016$  (2σ). A large error in the initial strontium isotope composition is due to high Rb/Sr ratios. The whole-rock Rb–Sr age of the biotite and amazonite–albite granites of the Urugudei Pluton is  $321 \pm 5$  Ma (Kostitsyn 2001). The same author summarized isotopic data for both intrusions and obtained a single isochron with an age of  $319 \pm 3$  Ma and (<sup>87</sup>Sr/<sup>86</sup>Sr)<sub>0</sub> =  $0.705 \pm 0.008$ .

**Tab. 1** Whole-rock composition of granites of the Kharagul and Urugudei plutons

Sample	KHR 612	KHR 649	KHR 637	KHR 603	UD 2005	Z 34	UD 2008
Plutons	Kharagul				Urugudei		
Phase	I phase	II phase			I phase	II phase	
SiO <sub>2</sub> (%)	72.83	74.53	77.51	73.87	75.23	70.69	72.02
TiO <sub>2</sub>	0.10	0.04	0.02	0.05	0.12	0.06	0.08
Al <sub>2</sub> O <sub>3</sub>	14.38	14.60	12.67	15.30	12.90	16.30	14.47
Fe <sub>2</sub> O <sub>3</sub>	0.62	0.02	0.17	0.32	0.52	0.72	0.72
FeO	1.25	0.98	0.53	0.26	1.16	0.35	0.35
MnO	0.08	0.07	0.06	0.08	0.06	0.06	0.07
MgO	0.05	0.05	0.05	0.05	0.10	0.05	0.10
CaO	0.60	0.20	0.05	0.05	0.40	0.30	0.65
Na <sub>2</sub> O	4.46	4.79	4.28	5.52	3.82	7.17	5.65
K <sub>2</sub> O	4.60	4.35	4.08	3.93	4.70	3.77	4.64
P <sub>2</sub> O <sub>5</sub>	0.02	0.02	0.02	0.02	0.03	0.03	0.09
LOI	0.76	0.55	0.46	0.46	0.69	0.32	0.64
Total	99.75	100.10	99.90	99.61	99.64	99.82	99.48
Li (ppm)	220	460	220	530	140	550	270
F	3000	3000	1500	5000	1000	5200	1400
Be	9.7	9.2	5.6	8.9	6.9	10.8	10.9
Zn	113	142	95	104	45	30	40
Ga	32	40	36	51	26	45	41
Ge	2.4	2.9	2.8	4.2	2.2	4.2	4.0
Rb	381	542	488	763	329	714	996
Sr	4	7	11	2	19	16	9
Y	41	24	165	50	43	20	50
Zr	368	75	102	86	134	46	74
Nb	73	56	36	64	62	44	39
Sn	22	41	19	48	6	13	14
Cs	20.0	28.0	15.0	28.0	12.0	56.0	51.0
Ba	11	22	51	11	68	62	42
La	50.00	3.05	14.40	9.60	31.00	2.52	13.40
Ce	116.00	10.00	33.00	28.00	68.00	10.10	41.00
Pr	12.60	1.39	5.50	3.77	7.90	1.59	5.30
Nd	47.00	5.60	23.00	14.50	29.00	6.70	19.00
Sm	9.00	1.70	6.10	3.67	7.00	2.70	6.40
Eu	0.09	0.02	0.05	0.02	0.16	0.05	0.04
Gd	8.30	1.80	8.00	3.47	7.40	2.96	6.30
Tb	1.23	0.35	1.48	0.64	1.25	0.70	1.31
Dy	7.60	2.60	10.40	4.69	8.30	5.10	9.30
Ho	1.53	0.57	2.39	1.03	1.68	1.09	1.91
Er	4.93	2.22	9.00	3.92	5.10	3.96	6.80
Tm	0.80	0.47	1.69	0.85	0.76	0.79	1.37
Yb	6.10	4.25	13.20	7.70	5.20	6.80	11.50
Lu	0.95	0.68	2.17	1.25	0.76	1.04	1.81
Hf	10.7	5.6	9.0	9.0	5.0	4.8	7.9
Ta	8.7	22.0	8.5	31.0	4.8	17.0	8.1
Pb	50.0	84.0	82.0	102.0	33.0	49.0	73.0
Th	31.0	19.0	27.0	21.0	56.0	9.3	13.6
U	10.1	3.3	8.8	4.1	7.8	2.1	6.3
K/Rb	101	67	70	43	119	44	39
Zr/Hf	34	13	11	10	27	10	9
La/Yb	8.2	0.7	1.1	1.2	6.0	0.4	1.2

**Tab. 2** Whole-rock composition of granites of the Bitu-Dzhida Pluton

Sample	BD 2417	BD 2421/1	BD 3202	BD 2443	BD 2438/1	BD 2414
Phase	I phase			II phase		
SiO <sub>2</sub> (%)	70.53	71.14	71.60	71.68	72.32	73.51
TiO <sub>2</sub>	0.30	0.30	0.27	0.31	0.24	0.19
Al <sub>2</sub> O <sub>3</sub>	14.47	14.93	14.99	14.76	14.04	14.15
Fe <sub>2</sub> O <sub>3</sub>	0.53	0.37	2.04	0.36	0.37	0.31
FeO	2.73	1.87	1.15	1.81	1.90	1.59
MnO	0.37	0.05	0.04	0.04	0.06	0.07
MgO	0.26	0.51	0.47	0.49	0.21	0.05
CaO	0.59	1.97	1.56	1.86	1.11	0.72
Na <sub>2</sub> O	4.10	3.99	4.34	3.76	4.00	4.18
K <sub>2</sub> O	3.21	3.21	3.80	3.36	4.15	4.14
P <sub>2</sub> O <sub>5</sub>	0.09	0.08	0.06	0.08	0.07	0.06
LOI	2.78	1.49	0.74	1.35	1.51	1.05
Total	99.95	99.89	100.01	99.85	99.97	100.02
Li (ppm)	328	174	138	140	200	272
F	7000	4700	2900	1900	2100	5400
Be	7.5	6.5	11.0	6.5	6.8	8.1
Zn	366	40	81	24	58	83
Ga	17	15	23	10	19	21
Ge	1.4	1.2	2.0	0.7	1.8	1.7
Rb	296	153	221	83	199	331
Sr	102	212	188	143	131	103
Y	14	11	23	9	35	60
Zr	132	143	177	90	164	162
Nb	18	14	35	9	39	46
Sn	25	8	13	3	8	18
Cs	12.0	8.2	13.4	3.6	9.9	11.0
Ba	595	703	685	491	449	361
La	23.49	24.68	25.66	17.83	34.96	36.41
Ce	46.01	46.43	55.77	33.75	68.80	72.18
Pr	5.00	4.87	5.82	3.75	7.90	8.42
Nd	17.85	18.88	21.79	12.96	29.00	37.24
Sm	3.89	3.23	4.42	2.61	6.99	8.32
Eu	0.50	0.67	0.61	0.49	0.63	0.50
Gd	2.72	2.48	4.46	1.99	6.40	8.49
Tb	0.40	0.32	0.68	0.28	1.15	1.46
Dy	2.36	1.91	4.04	1.56	7.05	9.38
Ho	0.45	0.38	0.79	0.31	1.41	1.98
Er	1.20	1.10	2.44	0.87	3.71	5.58
Tm	0.18	0.16	0.39	0.13	0.56	0.86
Yb	1.11	1.03	2.70	0.79	3.63	5.64
Lu	0.17	0.15	0.42	0.12	0.53	0.88
Hf	4.0	4.4	7.7	2.9	5.3	7.1
Ta	1.2	1.6	5.5	1.2	3.3	7.7
Pb	41.4	29.3	32.9	15.6	44.2	43.6
Th	10.9	12.2	17.8	7.7	24.0	25.1
U	3.3	3.5	5.1	2.7	7.6	7.6
K/Rb	90	175	143	337	174	104
Zr/Hf	33	33	23	31	31	23
La/Yb	21.2	24.0	9.5	22.6	9.6	6.5

## 4.2. Bitu-Dzhida Pluton

The rocks of all three intrusive phases of the Bitu-Dzhida Pluton are also classed as peraluminous granites (Fig. 7b) of the Li–F geochemical type. Silica, Al<sub>2</sub>O<sub>3</sub>, and Na<sub>2</sub>O contents increased during the formation of the multiphase intrusion. Compared with average composition of the continental crust (Antipin and Perepelov 2011), the granites of all intrusive phases have high F, Li, Sn contents, and the granites of the second and third phases are enriched in Ta, Nb, and Rb (Tab. 2). It should be noted that the granites of the early intrusive phase most closely approach the composition of the continental crust, whereas the rocks of the second and third phases show strongly differentiated distribution of many trace elements (Figs 8–9).

It is also important that the schists of the Bitu-Dzhida Fm. are similar in composition to the continental crust, except for small positive anomalies at Cs, B, and Li (Antipin and Perepelov 2011). The distribution of trace elements, including REE, in the rare-metal granites of the Bitu-Dzhida Pluton is consistent with the model of the fractional crystallization of primary magmas during the formation of granites of the second phase (Figs 6b and 7b). The model for genesis of the amazonite–albite granites of the third phase invokes fluid–magma liquid immiscibility in a fluorine-rich melt. Similar to the Kharagul and Urugudei plutons, a characteristic geochemical feature of the Bitu-Dzhida Pluton is a regular decrease in some indicator element ratios, K/Rb, Zr/Hf, and La/Yb, in the amazonite–albite granites of the final intrusive phases (Tab. 2, Fig. 8).

Sr–Nd–Pb isotopic data were obtained for all granitoids of the Late Paleozoic Bitu-Dzhida Pluton (Antipin and Perepelov 2011) (Tabs 4–5; Figs 11–12). They all yield comparable Nd model ages ( $T_{2DM}$ ) of ~ 1.0 to 1.3 Ga.

## 4.3. Janchivlan Pluton

Major- and trace-element analyses are shown in Tab. 3. Granites display an increase of silica (72–77 wt. % SiO<sub>2</sub>) from porphyritic coarse-grained biotite granite

to Li mica–albite granites. They have high SiO<sub>2</sub> and total alkalis (Fig. 6a). Granites are subaluminous to peraluminous with A/CNK values ranging from 1.02 to 1.33 (Fig. 7a). They are all highly evolved, but the three phases show distinct contents of silica. The granites of the first phase have ~ 72 wt. % SiO<sub>2</sub>, the second phase has a bimodal distribution of silica with maxima at 70 % and 74 wt. % SiO<sub>2</sub>, while the third phase granites typically contain ~ 75 wt. % SiO<sub>2</sub>.

The first- and second-phase granites of the Janchivlan Pluton have low CaO but high Al<sub>2</sub>O<sub>3</sub> and Fe/Mg, plotting into the high-K or shoshonitic fields (Gerel 1990). Their normative composition suggests minimum water pressure during crystallization of 1–0.5 kbar. On the Ab–Or–Qtz diagram, Li–F granites plot near the Ab corner (Kovalenko 1977; Gerel 1990).

Compared with the granites of the early phases, Li–F granites have lower CaO and MgO but higher total alkalis and Fe/Mg ratio. They have also lower Ba and Sr but higher Li, Nb, Rb, Y and Ga contents. Chondrite-normalized REE patterns are typical of evolved granites with strong negative Eu anomaly and enrichment in HREE for Li–F granites (Fig. 8d).

Major and trace elements show smooth trends going from granites of the first phase to those of the third phase. Among the trace elements Rb, Ta, Nb and Th increase, whereas Sr, Ti and Ba decrease. Rare-metal granites are enriched in Li, Be, Rb, Ta, Sn, W and F (Tab. 3).

Granites of the Janchivlan Pluton were emplaced in the marginal part of the Khentei Uplift and presumably had a genetic relation with granodiorite–gran-

Tab. 2 Continued

Sample Phase	BD 3502	BD 2437	BD 2436	BD 3241	BD 2427	BD 2406/1	BD 2406/2
SiO <sub>2</sub> (%)	73.24	73.70	74.16	75.07	78.05	70.37	78.02
TiO <sub>2</sub>	0.01	0.01	0.02	0.08	0.01	0.02	0.01
Al <sub>2</sub> O <sub>3</sub>	15.63	15.46	15.08	13.14	11.58	18.59	11.65
Fe <sub>2</sub> O <sub>3</sub>	1.01	0.14	0.16	1.79	0.20	0.09	0.21
FeO	0.57	0.69	0.80	1.22	1.03	0.47	1.06
MnO	0.08	0.07	0.08	0.04	0.15	0.02	0.14
MgO	0.07	0.05	0.05	0.05	0.05	0.05	0.05
CaO	0.04	0.05	0.07	0.30	0.05	0.08	0.08
Na <sub>2</sub> O	6.74	6.00	5.85	4.35	2.53	9.57	2.64
K <sub>2</sub> O	2.98	3.49	3.32	4.95	5.62	0.35	5.54
P <sub>2</sub> O <sub>5</sub>	0.02	0.01	0.01	0.01	0.01	0.01	0.01
LOI	0.30	0.35	0.41	0.22	0.70	0.35	0.64
Total	100.16	100.01	99.99	100.00	99.98	99.98	100.04
Li (ppm)	492	596	608	87	684	67	1136
F	2000	3200	2800	780	8800	1800	9500
Be	4.6	2.8	4.4	5.5	4.0	1.8	4.5
Zn	272	72	84	123	154	94	304
Ga	53	37	39	27	16	50	36
Ge	3.6	2.8	2.8	1.8	1.1	3.5	3.4
Rb	562	532	573	241	725	55	816
Sr	2.2	4.2	5.0	2.5	3.0	3.2	3.2
Y	16	6	6	11	13	2	26
Zr	275	216	213	292	86	239	84
Nb	63	113	350	66	192	21	451
Sn	21	21	114	4	49	10	105
Cs	16.2	7.3	7.8	5.6	3.9	2.5	14.4
Ba	54	11	15	76	10	11	11
La	2.81	1.43	0.56	6.48	2.11	0.23	5.37
Ce	12.46	5.58	2.54	17.22	7.33	1.31	24.03
Pr	1.85	0.77	0.37	2.20	1.17	0.25	3.44
Nd	6.80	2.61	1.22	8.71	3.40	0.81	10.52
Sm	2.72	0.98	0.56	2.15	1.12	0.42	4.37
Eu	0.01	0.01	0.01	0.14	0.01	0.00	0.02
Gd	2.49	0.66	0.46	2.13	0.96	0.31	4.48
Tb	0.72	0.19	0.17	0.43	0.32	0.10	1.19
Dy	5.93	1.64	1.62	3.11	2.42	0.84	9.42
Ho	1.28	0.37	0.42	0.70	0.52	0.20	2.07
Er	5.07	1.34	1.45	2.47	2.11	0.79	7.48
Tm	1.08	0.27	0.32	0.44	0.48	0.15	1.56
Yb	9.22	2.31	2.86	3.46	3.98	1.57	12.04
Lu	1.45	0.35	0.45	0.52	0.60	0.30	1.77
Hf	21.2	10.3	12.5	11.5	4.2	12.2	8.7
Ta	8.8	9.9	31.1	5.8	11.8	4.3	41.7
Pb	69.1	37.1	57.1	40.1	41.7	44.4	110.9
Th	50.4	30.3	41.2	19.5	39.3	42.6	91.4
U	11.3	9.7	8.7	7.2	2.9	16.6	36.5
K/Rb	44	55	48	171	65	53	57
Zr/Hf	13	21	17	25	20	20	10
La/Yb	0.3	0.6	0.2	1.9	0.5	0.1	0.4

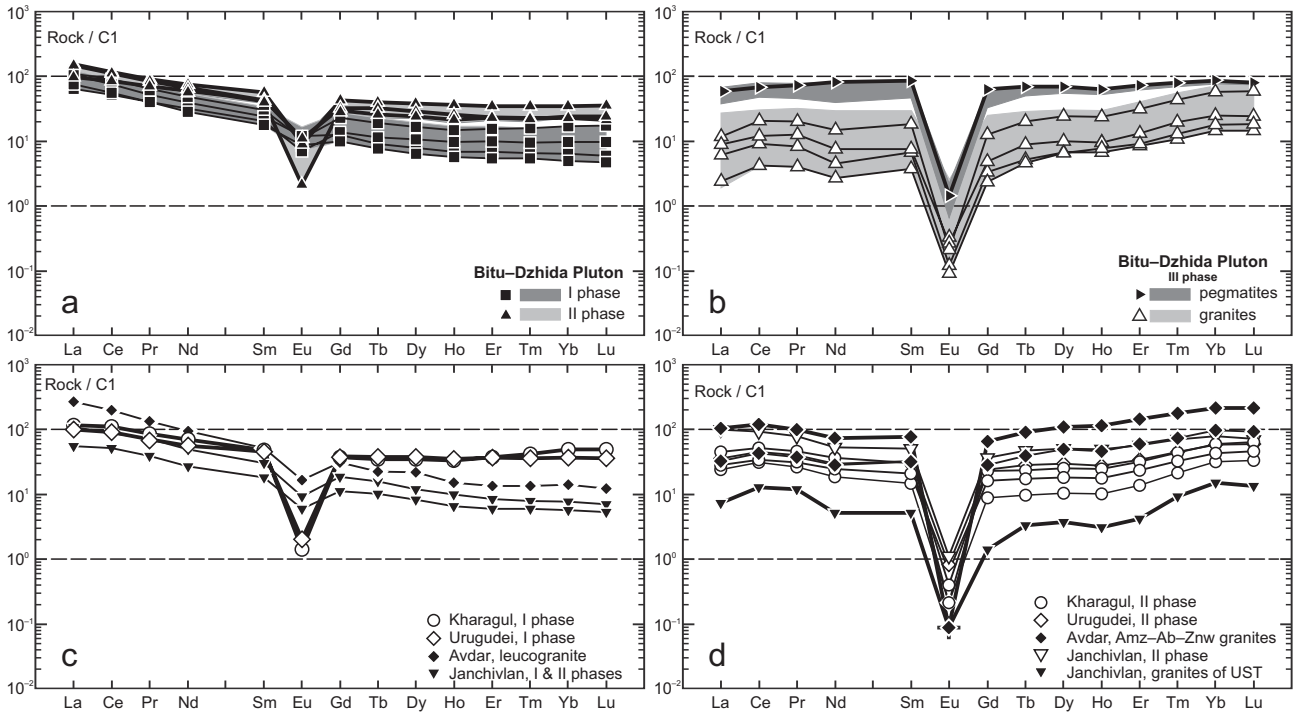


Fig. 8 Chondrite CI normalized (Sun and McDonough 1989) REE patterns in the granites of Central Mongolia and Baikal region.

ite batholiths (Koval 1998). The initial  $^{87}\text{Sr}/^{86}\text{Sr}$  ratios range from 0.7049 to 0.7044 for first and second phases, and from 0.7187 to 0.7306 for third-phase granites (Kovalenko et al. 1999). Albite–lepidolite granites show high initial  $^{87}\text{Sr}/^{86}\text{Sr}$  ratios due the error associated with high Rb/Sr ratios and influence of postmagmatic processes. The Li–F granites have very variable initial  $^{87}\text{Sr}/^{86}\text{Sr}$ . Their Y/

Nb ratios range between 1.2 and 7.0, and are thus characteristic of  $A_2$ -type granites (Gerel et al. 1999).

#### 4.4. The Avdar intrusion

On classification diagram (Fig. 6a) rocks of the Janchivlan Pluton and Avdar rare-metal intrusion show broad

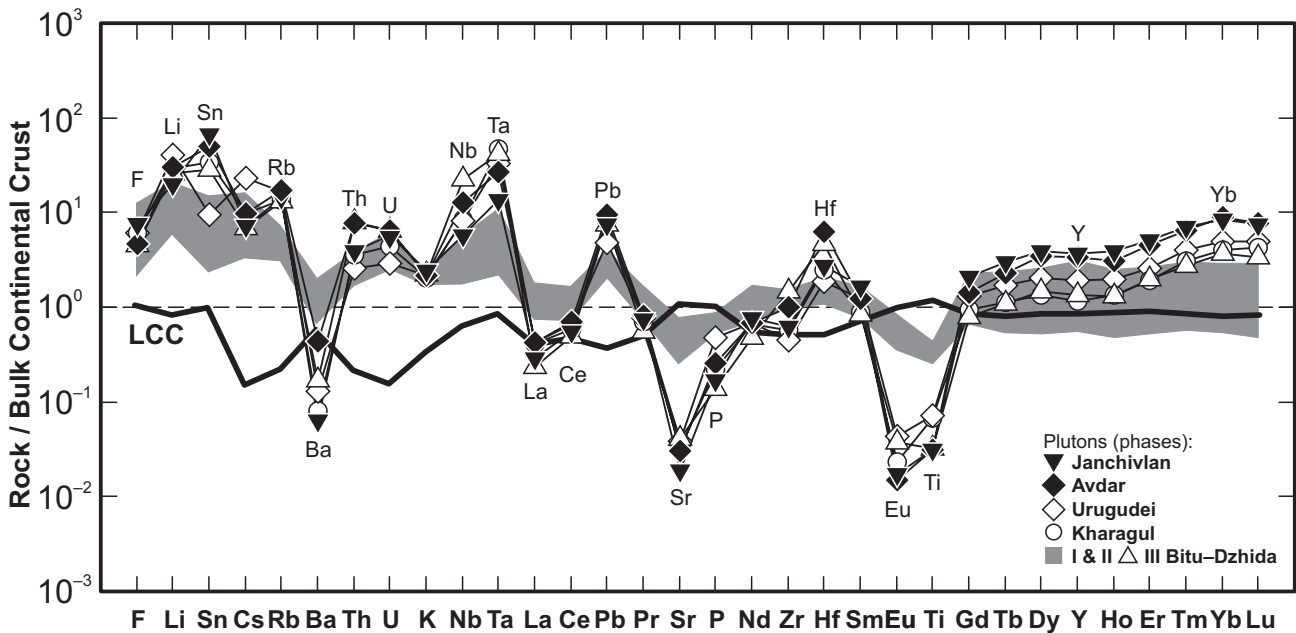


Fig. 9 Distribution of average trace-element contents in individual Li–F amazonite–albite granites of Baikal region and Central Mongolia. Normalized to the Bulk continental crust (Rudnick and Gao 2003).

variation in alkalinity from sub-alkaline to alkaline granites. The Early Mesozoic granite plutons have very variable potassium and sodium contents. However, most of these rare-metal granites have the ratio of  $K_2O/Na_2O$  close to 1. On the Shand diagram (Fig. 7a), granites of the Avdar Pluton fall in several fields according to their alkali and alumina balance.

The Avdar and Khoshutul plutons and comagmatic dike belt form a single Avdar-Khoshutul intrusive–dike rock series in the peripheral zone of the Early Mesozoic magmatism in the western part of Mongolia in the Mongol-Okhotsk Belt. The Avdar-Khoshutul intrusive–dike series is represented by different composition rocks from the early Khoshutul granitoid Pluton ( $224 \pm 10$  Ma) through alkaline syenite intrusions and numerous small subvolcanic dikes of granite–porphyry, and felsic ongonites to late rare-metal granites of the Avdar Pluton (209–212 Ma). In the dike belt near the Tsoh ul, dike of ongonite with topaz and fluorite was firstly found, and has the typical petrographic characteristics of these rare-metal subvolcanic rocks (Odgerel and Antipin 2009).

The Li–F granites of the final stage in the Avdar Pluton are typical crustal rocks with high initial  $^{87}Sr/^{86}Sr$  ratios (0.84–0.87), low initial  $\epsilon_{Nd}$  values (+1.2) and the Nd crustal residence  $T_{DM2}$  age of 0.9 Ga (Kovalenko et al. 1999).

## 5. Mineralization related to rare-metal granites

The intrusive–dike complex of the Khamar–Daban Range in the area of the Kharagul and Urugudei plutons, as well

as Utulik dike belts with elvans, ongonites, topazites, contains Sn and W veinlet–disseminated zones of the

**Tab. 3** Whole-rock composition of granites of the Janchivlan and Avdar plutons

Sample Plutons	J 1	J 2	J 4	J 4479	A 03–44	A 3260	A 3267B	A 3267A
	Janchivlan				Avdar			
Phase	I phase	II phase	III phase		I type		II type	
SiO <sub>2</sub> (%)	70.60	72.44	77.23	75.99	73.62	75.96	76.00	76.64
TiO <sub>2</sub>	0.27	0.24	0.08	0.02	0.20	0.02	0.01	0.02
Al <sub>2</sub> O <sub>3</sub>	15.11	14.46	12.50	13.03	13.65	13.75	13.32	13.58
Fe <sub>2</sub> O <sub>3</sub>	0.57	0.13	0.24	0.27	1.39	0.86	0.70	0.87
FeO	1.40	1.33	0.93	0.79	0.55	0.65	0.50	0.50
MnO	0.05	0.06	0.03	0.03	0.04	0.02	0.02	0.02
MgO	0.32	0.63	0.04	0.19	0.30	< 0.050	< 0.050	< 0.050
CaO	0.91	1.21	0.38	0.26	0.90	0.25	0.23	0.27
Na <sub>2</sub> O	3.61	3.55	3.88	4.32	4.12	5.31	2.86	4.86
K <sub>2</sub> O	5.96	4.54	4.50	4.39	4.60	3.52	6.60	3.54
P <sub>2</sub> O <sub>5</sub>	0.12	0.08	0.02	0.02	0.07	0.01	0.01	0.01
LOI	0.87	0.62	1.98	0.61	0.36	0.30	0.26	0.28
Total	99.79	99.29	101.81	99.91	99.80	100.04	100.06	100.11
Li (ppm)	135	148	400	318	40	358	449	570
F				4100	900	2600		
Be				6.7	1.7	21.3	8.4	8.0
Zn				366	16	177	250	277
Ga	21	20	29	41		48	43	46
Ge				3.6		5.2	6.3	6.1
Rb	377	315	870	701	160	1110	1986	1155
Sr	127	108	11	6	219	4	3	19
Y	30	14	113	47	22	66	33	57
Zr	165	105	155	83	298	183	70	157
Nb	15	11	46	46	23	66	161	132
Sn				115	3	24	215	217
Cs				14.0	3.0	10.5	24.6	21.8
Ba	500	303	97	30	648	11	11	763
La	25.53	12.94	35.48	5.67	62.89	8.26	6.01	7.70
Ce	53.64	31.30	80.04	24.02	121.11	29.28	17.94	24.86
Pr	6.61	3.59	9.66	3.67	12.38	3.23	2.35	3.51
Nd	22.22	12.24	30.23	15.46	43.22	13.75	7.18	10.83
Sm	4.42	2.70	7.26	6.51	7.58	4.21	2.50	3.77
Eu	0.52	0.34	0.13	0.02	0.92	0.01	0.00	0.01
Gd	3.66	2.18	7.09	7.65	6.11	4.82	2.93	4.18
Tb	0.57	0.36	1.65	1.80	0.81	0.91	0.59	0.91
Dy	2.94	2.02	11.97	14.02	5.33	7.74	5.15	8.32
Ho	0.54	0.36	2.77	2.97	0.81	1.62	1.10	1.76
Er	1.34	0.94	9.33	10.68	2.13	6.75	4.58	7.55
Tm	0.20	0.15	1.79	2.00	0.33	1.31	0.92	1.48
Yb	1.24	0.92	12.79	15.97	2.24	12.36	8.31	13.60
Lu	0.17	0.13	1.80	2.26	0.30	1.86	1.21	2.04
Hf				9.5	8.3	22.4	9.3	22.3
Ta				9.6	2.0	17.1	23.2	23.1
Pb	25.0	44.0	54.0	85.0	22.0	104.4	316.5	174.3
Th				22.1	38.4	36.4	19.3	28.0
U				7.6	2.7	5.1	10.5	11.0
K/Rb	132	120	43	52	240	26	28	26
Zr/Hf				9	36	8	8	7
La/Yb	20.6	14.1	2.8	0.4	28.1	0.7	0.7	0.6

**Tab. 4** Sr and Nd isotopic compositions of the granites of the Bitu-Dzhida Pluton

Sample	Phase	Rb	Sr	<sup>87</sup> Sr/ <sup>86</sup> Sr	2σ	<sup>87</sup> Sr/ <sup>86</sup> Sr(i)	Sm	Nd	<sup>143</sup> Nd/ <sup>144</sup> Nd	2σ	<sup>143</sup> Nd/ <sup>144</sup> Nd(i)	εNd(i)	T <sub>2DM</sub> (Ma)
BD 2417	I	296	102	0.742476	13	0.705187	3.89	17.85	0.512546	31	0.512280	0.80	1022
BD 2421/1	I	153	213	0.714462	10	0.705217	3.23	18.88	0.512398	7	0.512189	-0.97	1169
BD 3202	I	221	188	0.720624	2	0.705497	4.42	21.79	0.512492	5	0.512244	0.10	1080
BD 2414	II	331	103	0.747114	17	0.705785	8.32	37.24	0.512383	6	0.512110	-2.50	1297
BD 2438/1	II	199	131	0.724982	11	0.705526	6.99	29.00	0.512560	20	0.512266	0.52	1045
BD 2437	III	–	–	–	–	–	0.98	2.61	0.512543	13	0.512082	-3.05	1343
BD 3241	III	–	–	–	–	–	2.15	8.71	0.512378	8	0.512076	-3.17	1352
BD 3502	III	–	–	–	–	–	2.72	6.80	0.512555	21	0.512066	-3.38	1370
BD 2406/2	III	–	–	–	–	–	4.37	10.52	0.512576	7	0.512069	-3.32	1365

<sup>87</sup>Sr/<sup>86</sup>Sr and <sup>143</sup>Nd/<sup>144</sup>Nd values are measured isotopic ratios; <sup>87</sup>Sr/<sup>86</sup>Sr(i), <sup>143</sup>Nd/<sup>144</sup>Nd(i) and εNd(i) time-corrected values (assumed age 310 Ma); the εNd values were calculated using <sup>147</sup>Sm/<sup>144</sup>Nd = 0.1967 and <sup>143</sup>Nd/<sup>144</sup>Nd = 0.512638 for the present-day Chondrite Uniform Reservoir (CHUR) (Faure 1986). Nd model ages (Ma) were calculated based on a two-stage model (T<sub>2DM</sub>) of Keto and Jacobsen (1987). Nd model ages T<sub>2DM</sub> accepted only for samples with <sup>147</sup>Sm/<sup>144</sup>Nd < 0.14. All in-run errors of isotopic ratios (2σ) correspond to the last decimal of the reported ratios. The contents Rb, Sr, Sm and Nd are given in ppm (ICP-MS).

stockwork type, veins, and mineralized breccias. The early veins with Sn–W mineralization and mineralized breccias in the stockwork zone contain topaz, fluorite, and tourmaline. The late mineralization is rather uncommon and represented by quartz–feldspar–topaz–cryolite veins with disseminated cassiterite and wolframite (Chernov et al. 1988). Tantalum and tin occurrences in the Kharagul granites were found in separate zones with high tantalite–columbite and cassiterite contents. Tantalum and tin mineralization was also described from pegmatoid veins accompanying the intrusive complex of rare-metal granites.

Miarolitic pegmatites, Sn–W veins, Sn–W greisens, lepidolite–albite granites and albitites with Sn–Ta–Nb mineralization are known within the Janchivlan Pluton. Miarolitic pegmatites are associated with the phase I porphyritic coarse-grained biotite granites. More than 200 pegmatite bodies are known. They are composed of quartz, microcline, fluorite, topaz, beryl, mica (biotite, muscovite and zinnwaldite), and accessory minerals. A number of Sn–W mineralized prospects are associated with the phase II medium-grained muscovite–biotite granites in the Janchivlan Pluton. Ore-bearing veins are

small, rarely up to 1 m thick and 100 m long. Tourmaline and silica alterations are common. Greisen alteration is characteristic of granites of II and III phases. There are several different types of greisens, but the most common are quartz–tourmaline, quartz–topaz and quartz–muscovite types. Zinnwaldite-bearing greisen (zwitter) was described by Kovalenko et al. (1971).

Tantalum and Nb mineralization is associated with lepidolite–albite granites and albitites in the Urt Gozgor area. Lepidolite–albite granites stretch along the Ulaandavaa Fault for up to 3.5 km and are up to 800 m thick (Fig. 5). These granites have intrusive contacts with the host rocks, and granites of the phases I and III. Series of metasomatic rocks occur in the Urt Gozgor area: lepidolite albitites, amazonite albitites and quartz albitites (albite–lepidolite greisens) (Kovalenko et al. 1971). Albitites consist of albite (90 vol. %), microcline (3 %), quartz (3 %), lepidolite (2.5 %) and topaz (0.4 %). Lepidolite–albite granites and albitites contain accessory Ta–Nb minerals. Unidirectional solidification textures (UST) were recognized in the Urt Gozgor Sn occurrence. The UST are primary magmatic features, formed of parallel to subparallel bands of quartz crystals. These

**Tab. 5** Pb isotopic compositions of granites of the Bitu-Dzhida Pluton

Sample	Phase	U	Th	Pb	<sup>206</sup> Pb/ <sup>204</sup> Pb	2σ	<sup>207</sup> Pb/ <sup>204</sup> Pb	2σ	<sup>208</sup> Pb/ <sup>204</sup> Pb	2σ	<sup>206</sup> Pb/ <sup>204</sup> Pb(i)	<sup>207</sup> Pb/ <sup>204</sup> Pb(i)	<sup>208</sup> Pb/ <sup>204</sup> Pb(i)
BD 2417*	I	3.3	10.9	41.4	18.0711	10	15.5070	10	37.8038	30	17.8280	15.4942	37.5412
BD 2421/1*	I	3.5	12.2	29.3	18.2946	10	15.4960	10	37.9209	30	17.9258	15.4766	37.5037
BD 3202**	I	5.1	17.8	32.9	18.5135		15.5238		38.1505		18.0287	15.4983	37.6054
BD 2414*	II	7.6	25.1	43.6	18.3407	20	15.5010	20	37.9930	40	17.7982	15.4725	37.4133
BD 2438/1*	II	7.6	24.0	40.2	18.3667	20	15.4820	90	37.9089	40	17.7786	15.4511	37.3097
BD 2437*	III	9.7	30.3	37.1	18.0063	20	15.4619	20	37.8128	50	17.2023	15.4196	36.9978
BD 3241**	III	7.2	19.5	40.1	17.9818		15.4754		37.9063		17.4280	15.4463	37.4199
BD 3502**	III	11.34	50.4	69.1	18.1724		15.4919		38.0692		17.6626	15.4651	37.3372
BD 2406/1*	III	16.6	42.6	44.4	18.6321	8	15.5084	8	38.3496	20	17.4613	15.4469	37.3760
BD 2406/2**	III	36.5	91.4	110.9	18.4586		15.5044		38.2089		17.4329	15.4505	37.3770

<sup>206</sup>Pb/<sup>204</sup>Pb, <sup>207</sup>Pb/<sup>204</sup>Pb and <sup>208</sup>Pb/<sup>204</sup>Pb are measured isotopic ratios, \*corrected for mass fractionation and \*\*by dual isotope dilution method; <sup>206</sup>Pb/<sup>204</sup>Pb(i), <sup>207</sup>Pb/<sup>204</sup>Pb(i) and <sup>208</sup>Pb/<sup>204</sup>Pb(i) are initial (time-corrected) ratios respectively (assumed age 310 Ma). All in-run errors of isotopic ratios (2σ) correspond to the last decimal of the reported ratios. The contents of U, Th and Pb given in ppm.

textures were described by Kormilitsyn and Manuylova (1957), Povilaitis (1961), Bakumenko et al. (1981), Shannon et al. (1982) and Kirwin (2005). In general, these structures common in differentiated felsic intrusions in Mongolia are associated with Sn, Mo, porphyry Cu–Au, intrusion-related Cu and REE mineralizations, and are considered to be a useful indicator for volatile-rich intrusive complexes, at a distinct prospecting scale (Kirwin 2005).

Within the Avdar-Khoshutul intrusive–dike rock series are known occurrences of rare-metal mineralization in the western part of Avdar Pluton. It is Ta–Nb, and Sn–W-containing mineralized core and connected with spatial individual placers (Sn, W, Ta–Nb) that may be genetically linked to the granites of the Avdar Pluton.

## 6. Discussion

### 6.1. Geotectonic setting and geochemical evolution of studied rare-metal granites

This study reveals that all Late Paleozoic intrusions of rare-metal granites and accompanying subvolcanic dikes are confined to a single regional structure of the Khamar-Daban Ridge on the periphery of the large area of granitoid magmatism. The almost identical ages of the Kharagul, Urugudei, and Bitu-Dzhida plutons with the petrological and geochemical similarity of their rare-metal granites give grounds to assign them to a single geochemical type of Li–F granites and assume similar conditions of their formation.

The intraplate Late Paleozoic rare-metal granitic magmatism of the Khamar-Daban Ridge area shows a progressive increase in Na<sub>2</sub>O, F, Li, Rb, Cs, Sn, Be, Ta and Pb and a simultaneous decrease in FeO<sub>t</sub>, CaO, K<sub>2</sub>O, Ba, Sr, Zn, Zr, Th and U contents in the late intrusive phases (Tab. 2). A similar evolution was identified for the subvolcanic rocks, which confirms that both granites and related dikes belong to a single intrusive–dike complex (Antipin et al. 1999).

The Late Paleozoic rare-metal intrusions show broad variations in alkalinity. While the early biotite granites are mostly subalkaline, the rare-metal Li–F granites tend to be more alkaline, and fall at the border or even in the field of alkalic series (Fig. 6).

Early Mesozoic granites were emplaced after the continental collision and closure of the Mongol-Okhotsk Ocean which resulted in voluminous granitic magmatism producing batholiths in the Khentei Uplift's core as well as shallow small plutons outside the Mongol-Okhotsk Belt (e.g. Zonenshain et al. 1990; Koval 1998; Kovalenko et al. 1999). Yarmolyuk et al (2002) and Yarmolyuk et al. (2013) interpreted the Khentei Batho-

lith as a result of mantle plume activity in an intraplate tectonic setting.

Still, the evolutions of diachronous (Late Paleozoic vs. Early Mesozoic) rare-metal granites of the Baikal region and in Central Mongolia show a geochemical similarity (Figs 6–7). It is expressed by an increase in F, Li, Rb, Cs, Sn, Be, Ta and Pb and a decrease in Sr, Ba, Zn, Zr, Th and U contents in course of multiphase intrusions formation (Tabs 1–3; Figs 8–9).

On the other hand, there are also marked differences in K<sub>2</sub>O/Na<sub>2</sub>O ratios (wt. %). This ratio is greatly shifted in favor of Na<sub>2</sub>O for Late Paleozoic rare-metal granites, whereas their Mesozoic counterparts have K<sub>2</sub>O/Na<sub>2</sub>O close to, or greater than, unity. High Na contents in the Late Paleozoic rare-metal granites should be partly of metasomatic origin.

### 6.2. Unidirectional Solidification Textures (UST)

The magmatic mode of genesis of rare-metal Li–F granites is confirmed not only by geochemical data, but also by the presence of Unidirectional Solidification Textures (UST) in Bitu-Dzida and Urt Gozgor (Janchivlan) late phases. The UST zones are thought to be products of rhythmic precipitation of quartz and quartz + feldspar during periods of volatile over pressure within relatively small degassing felsic cupolas. The formation of UST is considered to be result of pulsating pressure changes across cotectic boundaries in the quartz–feldspar stability field. The quartz stability field expands with increasing pressure (Tuttle and Bowen 1958) and thus alternating bands of quartz and quartz plus feldspar are precipitated in cupolas as the cotectic boundary oscillates during pressure variation (Kirwin 2005).

In the Bitu-Dzhida intrusion were observed also heterogeneous solidification textures of liquid immiscibility (liquation) with segregation into two zones: fine-grained Ab–Kfs granite and coarse-grained Amz–Ab–Znw granite (Fig. 10a). The recombined composition of these zones is corresponding to an average composition of massive Amz–Ab–Znw granite of this pluton, as shown on the example of the REE pattern (Fig. 10b). This may indicate the parental rare-metal granitic magma later split into ore-bearing and barren phases.

### 6.3. Magma source

Initial εNd values ranging from –1.2 to –2.7 and two-stage Nd model ages (T<sub>2DM</sub>) older than 1.2 Ga were previously obtained for the Urugudei–Kharagul group of Late Paleozoic intrusions indicating that these plutons could have formed by melting of the local Precambrian continental crust (Kovalenko et al.

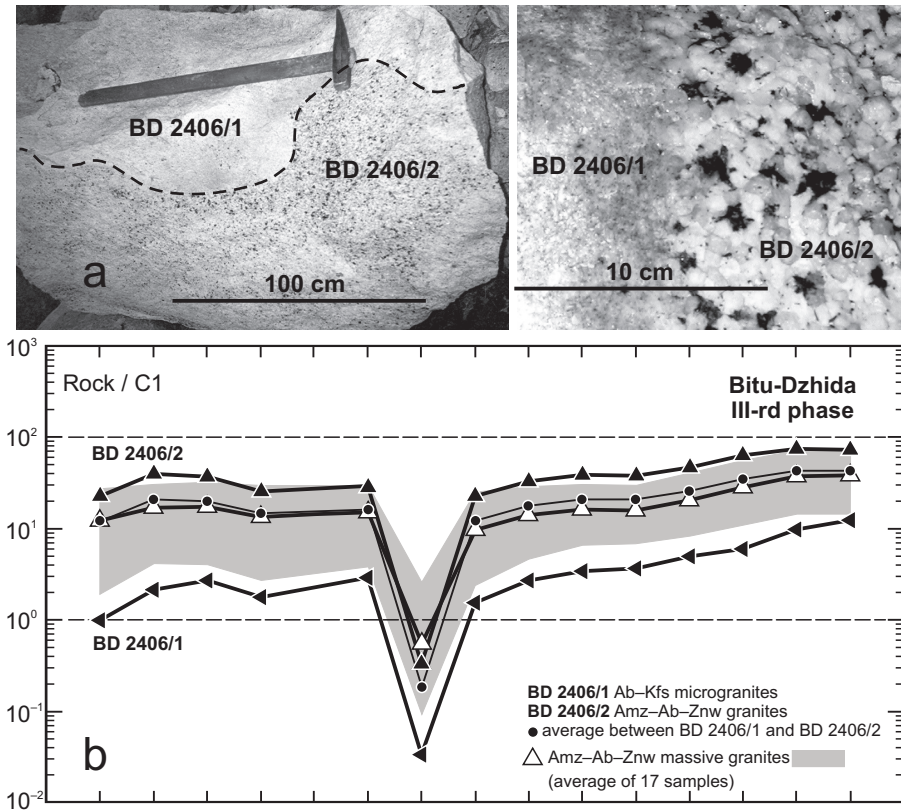
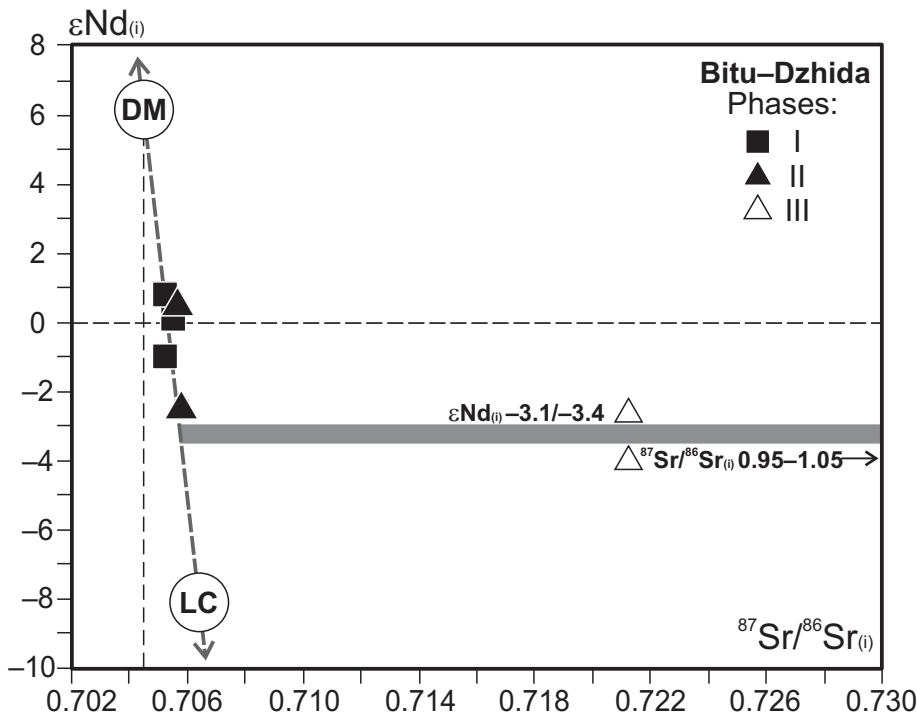


**Fig. 10** Heterogeneous solidification texture of the Bitu-Dzhida Pluton. Photo of sample (a) and chondrite-normalized (McDonough and Sun 1995) REE pattern (b).

1999). The whole-rock geochemical and isotope compositions point to the southern Baikal Precambrian continental crust as the most likely source (Makrygina 1981). The melting of the Precambrian continental crust of the Khamar-Daban Range could have been

caused by the heat and fluids derived from subalkaline (monzonitic) magmas, which preceded the occurrence of rare-metal granite magmatism in the region (Antipin et al. 1999).



#### 6.4. Origin of Li–F magma

Genesis of rare-metal granites is still being discussed. Beus et al (1962) interpreted these granites as metasomatically albitized (apogranites). Magmatic genesis of Li–F granites was proposed by Kovalenko et al. (1971) and proved in many world provinces (Haapala 1977; Christansen et al. 1988; Dostal and Chatterjee 1995; Raimbault et al. 1995; Antipin and Perepelov 2011). Origin of the rare-metal granite magma enriched in LILE components in both

**Fig. 11** Sr and Nd isotope characteristics of the Bitu-Dzhida granites. DM – Depleted Mantle, LC – Lower Crust (Kovalenko et al. 1999).

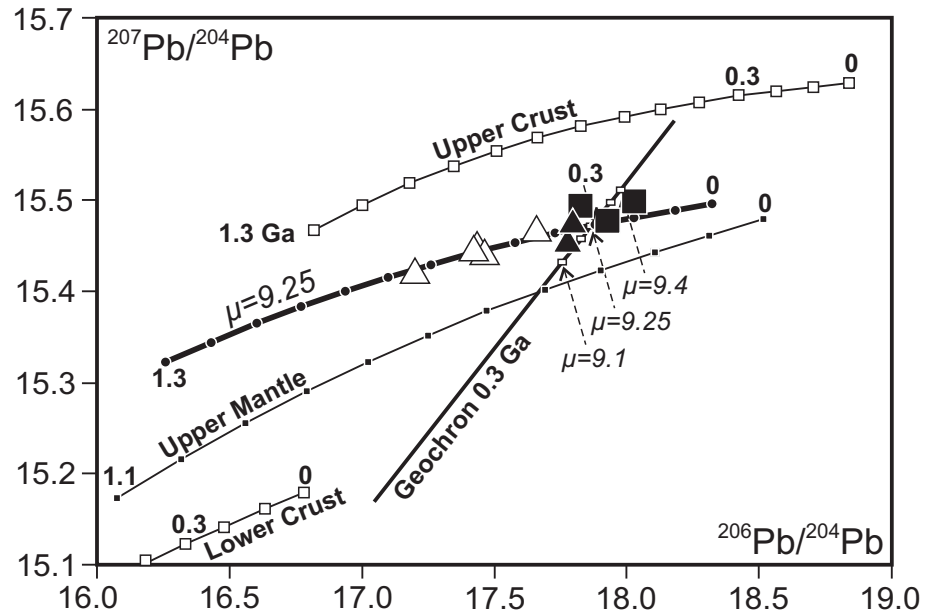


**Fig. 12** The whole-rock  $^{206}\text{Pb}/^{204}\text{Pb}$  vs.  $^{207}\text{Pb}/^{204}\text{Pb}$  plot for the Bitu-Dzhida Pluton. The Pb evolution curves for the main crustal and mantle reservoirs are after Kramers and Tolstikhin (1997). Lead evolution model for granitoids of the Bitu-Dzhida Pluton was calculated following Stacey and Kramers (1975).

Central Mongolia and the Baikal region can be explained using the model of Cuney and Barbey (2014) (Fig. 13).

This model assumes that during the granulite-facies metamorphism of mica-rich metasedimentary rocks, hydrous fluids enriched in  $\text{CO}_2$ , Cl and F are released capable of transporting many trace elements (Rb, Cs, Li, Sn and W). The same authors (Cuney and Barbey 2014) proposed that the  $\text{CO}_2$  fluid (the wave), resulting from the metamorphism of carbonates, or coming from the mantle, contributes to the extraction and transport of elements into shallower crust, into the region of anatexis melting. The relative rarity of rare-metal magmas can be explained by their association to the highly permeable shear zones in the crust. The authors acknowledged that elevated temperatures are a prerequisite of such a process.

In contrast to the model proposed by Cuney and Barbey, we suppose that the anatexis rare-metal magmas post-dated the granulite-facies metamorphism. The formation of high- $\text{CO}_2$ - $\text{H}_2\text{O}$ -F-containing “rare metal” fluid could have been a result of the influence of upwelling mantle diapir on felsic granulites. An alternative scenario represents delamination and sinking into the mantle of lower crustal blocks. Both scenarios are followed by subsequent destruction of the residual hydroxyl-containing minerals (Kovalenko et al 1999, 2004) (Fig. 13).

The formation of the granite magma enriched in Li, F, Rb, Sn, Pb, Th and U could have occurred by separating the F- and  $\text{H}_2\text{O}$ -enriched silicate melt produced due to breakdown of hydrous mafic minerals (e.g. mica) in lower crust, followed by anatexis at higher crustal levels. The rise of the F,  $\text{H}_2\text{O}$ ,  $\text{CO}_2$  and LILE-rich high-temperature fluid along zones of increased permeability could have triggered a low-degree melting of the overlying crust and formation of rare-metal granitic melts. Fraction of the

fluid in the granitic melts would consistently increase with decreasing degree of anatexis melting, yielding the most enriched F, Li, Rb, U and Th granitic magmas.

Assumed importance of  $\text{CO}_2$ -rich fluid in transfer of trace elements is confirmed by forming of REE-carbonate in the rare metal granites. For example, in the Bitu-Dzhida Pluton, the Phase I granites contain accessory mineralization of REE-carbonates (parisite, synchysite) and the Phase III Amz-Ab-Znw granites Fe-Mn-containing calcite.

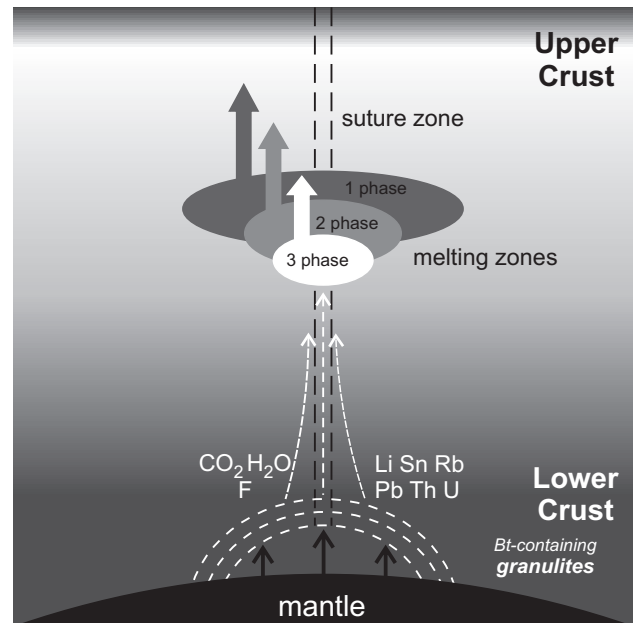


**Fig. 13** The conceptual model of the genesis of the rare-metal granitic magma due to the crust-mantle interaction (modified from Cuney and Barbey 2014).

Lead isotopic characteristics of rare-metal granites in the Bitu-Dzhida Pluton indicate the relatively old lower crust as a source of the LILE-enriched fluids. The most clearly is this shown in the granites of the final phase (Fig. 12), which were formed in the end of anatectic melting and were thus fluid-enriched.

Presence of UST and variation in our geochemical data also support the magmatic genesis of granites from the Janchivlan Pluton. The elevated alkalinity and low initial  $^{87}\text{Sr}/^{86}\text{Sr}$  ratios (0.704) for the first- and second-phase granites suggest their deep crustal origin. Low initial  $^{87}\text{Sr}/^{86}\text{Sr}$ , close to the mantle values, are characteristic of many rare-metal granites (Kostitsyn 2001).

There is a significant increase in Nb, Y and Zr and a decrease in Ba and Sr from the first- to the third-phase granites for multiphase plutons like the Janchivlan. This variation could be due to the fractional crystallization, especially the increase of Rb (the average K/Rb ratios rise from 170 for the first phase, through 158 for the second and 63 for the third-phase leucogranites, to 19–13 in Li–F granites)

Granites of the third phase are highly fractionated with complex magmatic and metasomatic signature. The source of F and rare elements was probably magmatic. At the late- magmatic and early postmagmatic stage, there was a new inversion of magmatic fluids. In later phases of the rare-metal intrusions practically exhausted the potential of fractional crystallization, and the microcline–albite facies formed with maximum concentrations of LIL and ore elements. Total REE fall accompanied by an increase in HREE, similar to albitized granite and albitites.

However, the comparative geochemical analysis of the calc-alkaline and Li–F granites suggests that the crustal anatexis alone could not have produced magmas with the geochemical characteristics of the rare-metal granites. Clearly, any subsequent fluid–magmatic fractionation would have resulted in extensive enrichment in F and many trace elements as observed in Li–F granites and their subvolcanic analogues (ongonites), presumed products of the residual magmas crystallization. In the recent study of ongonites, Dostal et al. (2015) have shown that they underwent subsolidus exchange with deuteric fluids which led to the origin of secondary Li–Fe-rich micas enriched in rare metals.

In any case, the presence of UST shows that the apical parts of the felsic intrusions formed at relatively high temperatures. Indeed, temperatures of 780–800 °C were obtained based on biotite  $\text{Fe}/(\text{Fe} + \text{Mg})$  ratio and fugacity of oxygen ( $f\text{O}_2$ ) (Wones and Eugster 1965) as well as zircon saturation thermometry (Watson and Harrison 1983) (Gerel 1990). These data are in a good agreement with fluid inclusions study of Koval (1998) for Mesozoic granitoids in the Mongol-Okhotsk Belt yielding 940 °C

for rare-metal granites and 860 °C for Li–F granites, e.g. microcline–albite ones. At these conditions, volatile activity increased and resulted in formation of UST in the relatively closed system. Postmagmatic stage was then responsible for the rare-metal mineralization.

Volatiles are considered to play an important role in the petrogenesis of the Li–F granites. Highly evolved granites with Li–F facies have been described from many rare-metal provinces in the world (e.g. Kovalenko et al. 1971; Gerel 1990; Štemprok 1991; Taylor 1992; Dostal and Chatterjee 1995; Raimbault et al. 1995; Reyf et al. 1999; Antipin et al. 2001; Kostitsyn 2001; Linnen and Cuney 2005; Badanina et al. 2010; Gu et al. 2010).

For example, in the Janchivlan Pluton, the F content varies from 0.17 in the first phase, 0.19 in the second, 0.28–0.39 in the third, and up to 1.03–2.00 % in the ongonites (Kovalenko et al. 1971; Koval 1998). The abundance of F resulted in a highly mobile magma capable of reaching high crustal levels (Kovalenko 1977).

The Li–F granites always occur in the highest level of leucocratic cupolas or at the inner contacts of multiphase plutons (Kovalenko et al. 1971; Gerel 1990). The presence of late-stage F-rich fluid was also important for the metasomatic processes. The Li–F granites were followed by albitites and microclinites, greisens and quartz veins with Sn, W and Ta–Nb mineralization.

## 7. Conclusions

Late Paleozoic and Early Mesozoic rare-metal granitoids of Central Mongolia and Baikal region form small (up to 10 km<sup>2</sup>) multiphase intrusions, sharing similar modal composition, petrology and whole-rock geochemistry. Their geochemical evolution shows that they belong to a common geochemical type of Li–F granites. It is expressed by a progressive increase in F, Li, Rb, Cs, Sn, Be, Ta, Pb and drop in Sr, Ba, Zn, Zr, Th and U during the formation of these multiphase intrusions. The geochemical data suggest the magmatic genesis of rare-metal Li–F granites, and the process of magma differentiation leading to the formation of topaz-bearing amazonite–albite and lepidolite–albite granites.

In addition, metasomatic albitites, microclinites, zwitter and muscovite greisens are associated with the rare-metal mineralization. Rare-metal Li–F granites show a characteristic geochemical signature, independent of their age as well as the composition of their Precambrian and Phanerozoic metasedimentary country rocks. Based on the isotopic and whole-rock geochemical data, the initial generation of rare-metal Li–F magmas could have occurred in the lower continental crust during the granulite-facies metamorphism of biotite-rich metasediments.

The genetic scenario assumes an influence of mantle diapir on the crustal rocks that underwent the granulite-facies metamorphism at low pressures; an alternative is delamination and sinking into the mantle of lower crustal blocks, both causing destruction of hydroxyl-bearing minerals. In either case, the CO<sub>2</sub>-H<sub>2</sub>O-F-rich fluids would have induced anatectic crustal melting and formation of rare-metal magmas. Later, this magma could have undergone a long and deep magmatic differentiation leading to an enrichment of residual magmas and fluids in lithophile elements and fluorine at the late- and post-magmatic stages.

Rare-metal Li-F granites of studied provinces have intraplate origin and geochemically differ from the Early Paleozoic collisional granitoids. In contrast to the rare-metal intrusions, monzodiorites and quartz monzonites form large plutons in the near periphery of the Angara-Vitim Batholith and occur in the composite dikes of belt consisting of intrusions and dikes. Rare-metal granites formed on the periphery of the Late Paleozoic and Early Mesozoic magmatic belts, often as a part of intrusive-dike complexes.

*Acknowledgements.* Research has been supported by the RNF grant 15-17-10010. The authors are very grateful to the handling editor K. Schulmann and editor in chief V. Janoušek, as well as two anonymous reviewers for valuable and very constructive comments.

## References

- ANTIPIN VS (1977) Petrology and Geochemistry of Granitoids of Various Depth Facies. Nauka, Novosibirsk, pp 1–160 (in Russian)
- ANTIPIN VS, PEREPELOV AB (2011) Late Paleozoic rare-metal granitoid magmatism of the southern Baikal region. *Petrology* 19: 370–381
- ANTIPIN VS, SAVINA EA, MITICHKIN MA, PERELYAEV VI (1999) Rare-metal lithium-fluorine granites, ongonites and topazites of the South Baikal region. *Petrology* 7: 145–155 (in Russian)
- ANTIPIN VS, HALLS C, SELTMANN R (2001) Elvan and ongonite magmas with associated rare-metal mineralization. In: PIESTRZYŃSKI et al. (eds) *Mineral Deposits at the Beginning of the 21<sup>st</sup> Century*. Proceedings of the Joint Sixth biennial SGA–SEG Meeting, Kraków, Poland. Balkema, Lisse, pp 359–362
- ANTIPIN VS, HALLS C, MITICHKIN MA, SCOT P, KUZNETSOV AN (2002) Elvan of Cornwall (England) and southern Siberia as subvolcanic counterparts of subalkalic rare-metal granites. *Rus Geol Geoph* 9: 847–857
- BADANINA EV, VEKSLER IV, THOMAS R, SYRITSO LF, TRUMBULL RB (2010) Magmatic evolution of Li-F, rare metal granites: a case study of melt inclusions in the Khangilay Complex, Eastern Transbaikalia (Russia). *Chem Geol* 210: 113–133
- BAKUMENKO LT, KASUKHIN ON, KOSALS JA, LKHAMSUREN J (1981) On the genesis of rhythmically banded textures in granitoids. *Dokl Akad Nauk SSSR* 260: 444–448 (in Russian)
- BEUS AA, SEVEROV VA, CITNIN AA, CUBBOTIN KD (1962) Albitized and Greisenized Granites (Apogranites). Academy of Sciences of USSR, Moscow, pp 1–196
- CHERNOV BS, GETMANSKAYA TI, MEDNIKOV NI (1988) On cryolite-tin-tungsten-silver mineralization. *Geol Rudn Mestorozhd* 1: 69–76
- CHRISTIANSEN EH, STUCKLESS JS, FUNKHOUSER MJ, HOWELL KA (1988) Petrogenesis of rare-metal granites from depleted crustal sources – an example from the Cenozoic of western Utah, USA. In: TAYLOR RP, STRONG DF (eds) *Recent Advances in the Geology of Granite-Related Mineral Deposits*. Canadian Institute of Mining and Metallurgy Special Volume 39: pp 307–325
- COLLINS WJ, BEAMS SD, WHITE AR, CHAPPELL BW (1982) Nature and origin of A-type granites with particular reference to southeastern Australia. *Contrib Mineral Petrol* 80: 189–200
- CUNEY M, BARBEY P (2014) Uranium, rare metals, and granulite-facies metamorphism. *Geosci Front* 5: 729–745
- DONSKAYA TV, GLADKOCHUB DP, MAZUKABZOV AM, IVANOV AV (2013) Late Paleozoic–Mesozoic subduction-related magmatism at the southern margin of the Siberian Continent and the 150 million-year history of the Mongol-Okhotsk Ocean. *J Asian Earth Sci* 62: 79–97
- DOSTAL J, CHATTEJEE AK (1995) Origin of topaz-bearing and related peraluminous granite of the Late Devonian Davis Lake Pluton, Nova Scotia, Canada: crystal versus fluid fractionation. *Chem Geol* 123: 67–88
- DOSTAL J, KONTAK DJ, GEREL O, SHELLNUTT JG, FAVEK M (2015) Cretaceous ongonites (topaz-bearing albite-rich microleucogranites) from Ongon Khaikhan, Central Mongolia: products of extreme magmatic fractionation and pervasive metasomatic fluid: rock interaction. *Lithos* 236–237: 173–189
- FAURE G (1986) *Principles of Isotope Geology*, 2<sup>nd</sup> edn. John Wiley and Sons, New York, pp 1–589
- FROST BR, BARNES CG, COLLINS WJ, ARCULUS RJ, ELLIS DJ, FROST CD (2001) A geochemical classification for granite rocks. *J Petrol* 42: 2033–2048
- GALER SJG (1999) Optimal double and triple spiking for high precision lead isotopic measurement. *Chem Geol* 157: 255–274
- GEREL O (1990) Petrology, Geochemistry and Mineralisation of Mesozoic Subalkaline Granites in Mongolia. Unpublished Doctor of Sciences thesis, Vinogradov Institute of Geochemistry, Irkutsk, pp 1–395 (in Russian)

- GEREL O, KANISAWA S, ISHIKAWA K (1999) Petrological characteristics of granites from the Avdrant and Janchivlan plutons, Khentei Range, Central Mongolia. *Problems of geodynamics and metallogeny of Mongolia*. Transactions 13: 34–39
- GU LX, ZHANG ZZ, WU CZ, GOU XQ, LIAO JJ, YANG H (2010) A topaz- and amazonite-bearing leucogranite pluton in eastern Xinjiang, NW China and its zoning. *J Asian Earth Sci* 42: 885–902
- HAAPALA I (1977) Petrography and geochemistry of the Eyräjoki stock, a rapakivi-granite complex with greisen-type mineralization in south-western Finland. *Bull Geol Surv Finland* 290: 122–133
- JAHN BM, CAPDEVILA R, LIU D, VERNOV A, BADARCH G (2004) Sources of Phanerozoic granitoids in the transect Bayanhongor-Ulan Baator, Mongolia: geochemical and Nd isotopic evidence, and implications of Phanerozoic crustal growth. *J Asian Earth Sci* 23: 629–653
- JAHN BM, LITVINOVSKY BA, ZANVILEVICH AN, REICHOV M (2009) Peralkaline granitoid magmatism in the Mongolian–Transbaikalian Belt: evolution, petrogenesis and tectonic significance. *Lithos* 113: 521–539
- KETO LS, JACOBSEN SB (1987) Nd and Sr isotopic variations of Early Paleozoic oceans. *Earth Planet Sci Lett* 84: 27–41
- KIMURA JI, TAKAKU Y, YOSHIDA T (1995) Igneous rock analysis using ICP-MS with internal standardization, isobaric ion overlap correction, and standard addition methods. *Sci Rep Fukushima Univ* 56: 1–12
- KIRWIN DJ (2005) Unidirectional solidification textures associated with intrusion related Mongolian mineral deposits. In: SELTMANN R, GEREL O, KIRWIN DJ (eds) *Geodynamics and Metallogeny of Mongolia with Emphasis on Copper and Gold Deposits*. CERCAMS, London, pp 63–85
- KORMILITSYN VS, MANUYLOVA MM (1957) Rhythmic banded quartz porphyry. Bugdava Mountain, southwest Transbaikalian region. *Transact Mineral Soc, 2<sup>nd</sup> Series, Part 86*: 355–364 (in Russian)
- KOSTITSYN YA (2001) Sources of rare metals in peraluminous granites: a review of geochemical and isotopic data. *Geochem Int* 39: 43–59
- KOVAL PV (1998) Regional Geochemical Analysis of Granitoids. Siberian Branch of Russian Academy of Sciences Novosibirsk, pp 1–491 (in Russian)
- KOVALENKO VI (1977) Petrology and Geochemistry of Rare Metal Granitoids. Nauka, Novosibirsk, pp 1–206 (in Russian)
- KOVALENKO VI (1978) The genesis of rare-metal granitoids and related ore deposits: In: ŠTEMPROK M (ed) *Metalization Associated with Acid Magmatism vol. 3*. Czech Geological Survey, Prague, pp 235–248
- KOVALENKO VI, KOVALENKO NI (1976) Ongonites (Topaz-bearing Quartz Keratophyres): Subvolcanic Analogues of Rare-Metal Lithium–Fluorine Granites. Nauka, Moscow, pp 1–127 (in Russian)
- KOVALENKO VI, KUZMIN, MI, ZONENSHAIN LP, NAGIBINA MS, PAVLENKO AS, VLADYKIN NV, TSEDEN TS, GUNDSAMBUU TS, GOREGLYAD AV (1971) Rare-metal granitoids in Mongolia: petrology, distribution of rare elements. *Transactions* 5: 1–239 (in Russian)
- KOVALENKO VI, YARMOLYUK VV, BOGATIKOV OA (1995) Magmatism, Geodynamics, and Metallogeny of Central Asia. MIKO – Commercial Herald Publisher, Moscow, pp 1–274
- KOVALENKO VI, KOSTITSYN YA, YARMOLYUK VV, BUDNIKOV SV, KOVACH VP, KOTOV AB, SAL'NIKOVA EB, ANTIPIN VS (1999) Magma sources and the isotopic (Sr and Nd) evolution of Li–F rare-metal granites. *Petrology* 7: 383–409
- KOVALENKO VI, YARMOLYUK VV, KOVACH VP, KOTOV AB, KOZAKOV IK, SAL'NIKOVA EB, LARIN AM (2004) Isotopic provinces, mechanism of generation and sources of the continental crust in the Central Asian mobile belt: geological and isotopic evidence. *J Asian Earth Sci* 23: 605–627
- KRAMERS JR, TOLSTIKHIN IN (1997) Two terrestrial lead isotope paradoxes, forward transport modelling, core formation and the history of the continental crust. *Chem Geol* 139: 75–110
- KROGH T (1973) A low contamination method for hydrothermal decomposition of zircon and extraction of U and Pb for isotope age determinations. *Geochim Cosmochim Acta* 37: 485–494
- LI S, WANG T, WILDE SA, TONG Y (2013) Evolution, source and tectonic significance of Early Mesozoic granitoid magmatism in the Central Asian Orogenic Belt (central segment). *Earth-Sci Rev* 126: 206–234
- LINNEN RL, CUNNEY M (2005) Granite-related rare-element deposits and experimental constraints on Ta–Nb–W–Sn–Zr–Hf mineralization. In: LINNEN RL, SAMSON IM (eds) *Rare-Element Geochemistry and Mineral Deposits*. Geological Association of Canada Short Course Notes 17: pp 45–68
- LOISELLE MC, WONES DS (1979) Characteristics and origin of anorogenic granites. *Geological Society of America, Abstracts with Programs* 11: 468
- MAKRYGINA VA (1981) Geochemistry of Regional Metamorphism and Ultrametamorphism of Moderate and Low Pressure. Nauka, Novosibirsk, pp 1–200 (in Russian)
- MCDONOUGH WF, SUN S-s (1995) The composition of the Earth. *Chem Geol* 120: 223–254
- ODGEREL D, ANTIPIN VS (2009) Avdar-Khoshutula intrusive-dyke series of calc-alkaline, alkaline and rare metal granitoids of Central Mongolia. *Izvestiya of Siberian Department of Russian Academy of Natural Sciences. Geology, Prospect and Survey of Ore Deposits* 1(34): 58–68 (in Russian)
- PIN C, ZALDUEGUI JFS (1997) Sequential separation of light rare-earth elements, thorium and uranium by miniaturized extraction chromatography: application to isotopic analyses of silicate rocks. *Anal Chem Acta* 339: 79–89

- PIN C, DANIELLE B, BASSIN C, POITRASSON F (1994) Concomitant separation of strontium and samarium–neodymium for isotopic analysis in silicate samples, based on specific extraction chromatography. *Anal Chem Acta* 299: 209–217
- POVILAITIS MM (1961) About rhythmic zonality of some granitic bodies. *Izv Akad Nauk SSSR, Ser Geol* 2: 35–50 (in Russian)
- RAIMBAULT L, CUNEY M, AZENCOTT C, DUTHOU JL, JORON JL (1995) Geochemical evidence for a multistage magmatic genesis of Ta–Sn–Li mineralization in the granite at Beauvoir, French Massif Central. *Econ Geol* 90: 548–576
- REYF F, SELTMANN R, ZARAIISKY G, FEDKIN A (1999) Inclusion derived data on features of tantalite-saturated melt and its responsibility for the formation of the Orlovka tantalum deposit, Transbaikalia. *Terra Nostra* 99/6: 250–252
- RUDGE JF, REYNOLDS BC, BOURDON B (2009) The double spike toolbox. *Chem Geol* 265: 420–431
- RUDNICK RL, GAO S (2003) Composition of the Continental Crust. In: HOLLAND H.D, TUREKIAN KK (eds) *Treatise on Geochemistry* vol. 3, The Crust. Elsevier-Pergamon, Oxford, pp 1–64
- SHANNON JR, WALKER BM, CARTEN RB, GERAGHTY EP (1982) Unidirectional solidification textures and their significance in determining relative ages of intrusions at the Henderson Mine, Colorado. *Geology* 10: 293–297
- SHAND SJ (1943) *The Eruptive Rocks*, 2<sup>nd</sup> edn. John Wiley, New York, pp 1–444
- SUN SS, McDONOUGH WF (1989) Chemical and isotopic systematics of oceanic basalts: implications for mantle composition and processes. In: SAUNDERS AD, NORRY MJ (eds) *Magmatism in the Ocean Basins*. Geological Society of London Special Publications 42: pp 313–345
- STACEY JS, KRAMERS JD (1975) Approximation of terrestrial lead isotope evolution by a two-stage model. *Earth Planet Sci Lett* 26: 207–221
- ŞENGÖR AMC, NATAL'IN BA, BURTMAN VS (1993) Evolution of Altaid tectonic collage and Paleozoic crustal growth in Eurasia. *Nature* 364: 299–307
- ŠTEMPROK M (1991) Ongonite from Ongon Khairkhan, Mongolia. *Mineral Petrol* 43: 255–273
- ŠTEMPROK M, SELTMANN R (1994) The metallogeny of the Erzgebirge (Krušné Hory). In: SELTMANN R, KÄMPF H, MÖLLER P (eds) *Metallogeny of Collisional Orogens*. Czech Geological Survey, Prague, pp 61–69
- TAUSON LV (1977) The geochemical types of granitoids and their potential ore capacity. Nauka, Moscow, pp 1–280 (in Russian)
- TAYLOR RP (1992) Petrological and geochemical characteristics of the Pleasant Ridge zinnwaldite–topaz granite, southern New Brunswick and comparisons with other topaz-bearing felsic rocks. *Canad Mineral* 30: 895–921
- TISCHENDORF G, PALCHEN W (1985) Zur klassifikation von Granitoiden. *Z Geol Wiss* 13: 615–627
- TUTTLE OF, BOWEN NL (1985) Origin of granite in the light of experimental studies in the system NaAlSi<sub>3</sub>O<sub>8</sub>–KAlSi<sub>3</sub>O<sub>8</sub>–SiO<sub>2</sub>–H<sub>2</sub>O. Geological Society of America, *Memoirs* 74, pp 1–153
- USHAKOV VI, BOGUSLAVSKY IS (1969) Geological position, structure and composition of the albitites of Buural-Khangai Massif (Central Mongolia) Notes of NIIGA. *Regional Geology* 14: 71–74 (in Russian)
- VASIL'eva IE, SHABANOVA EV (2012) Arc Atomic-Emission Analysis in Geochemical Research. In: *Inorganic Materials*. English translation of selected articles from Zavodskaya Laboratoriya. *Diagnostika Materialov* 78: pp 14–24
- WATSON EB, HARRISON TM (1983) Zircon saturation revisited: temperature and composition effects in a variety of crustal magma types. *Earth Planet Sci Lett* 64: 295–304
- WHALEN JB, CURRIE KL, CHAPPELL BW (1987) A-type granites: geochemical characteristics, discrimination and petrogenesis. *Contrib Mineral Petrol* 95: 407–419
- WINDLEY BF, ALEXEIEV D, XIAO W, KRÖNER A, BADARCH G (2007) Tectonic models for accretion of the Central Asian Orogenic Belt. *J Geol Soc, London* 164: 31–47
- WONES DR, EUGSTER HP (1965) Stability of biotite: experiment, theory and application. *Amer Miner* 50: 1228–1271
- YARMOLYUK VV, KOVALENKO VI (2003) Batholiths and geodynamics of batholith formation in the Central Asian Fold Belt. *Rus Geol Geoph* 40: 1305–1320 (in Russian)
- YARMOLYUK VV, KOVALENKO VI, SAL'NIKOVA EB, BUDNIKOV SV, KOVACH VP, KOTOV AB, PONOMARCHUK VA (2002) Tectono-magmatic zoning, magma sources, and geodynamics of the Early Mesozoic Mongolo-Transbaikalian magmatic area. *Geotectonics* 36: 293–311
- YARMOLYUK VV, KUZMIN MI, KOZLOVSKY AM (2013) Late Paleozoic–Early Mesozoic within-plate magmatism in north Asia: traps, rifts, giant batholiths, and the geodynamics of their origin. *Petrology* 21: 101–126
- YARMOLYUK VV, KUZMIN MI, ERNST RE (2014) Intraplate geodynamics and magmatism in the evolution of the Central Asian Orogenic Belt. *J Asian Earth Sci* 93: 158–179
- ZONENSHAIN LP, KUZMIN MI, NATAPOV LM (1990) *Tectonics of Lithosphere Plates of the Territory of USSR*, Vol. 2. Nedra, Moscow, pp 1–334 (in Russian)

